Non-Invasive Mobile Raman and pXRF Analysis of Armorial Porcelain with the Coat of Arms of Louis XV and Others Enamelled in Canton: Analytical Criteria for Authentication

Philippe Colomban, Gulsu Simsek Franci, Xavier Gallet

heritage

MDPI

Article

Non-Invasive Mobile Raman and pXRF Analysis of Armorial Porcelain with the Coat of Arms of Louis XV and Others Enamelled in Canton: Analytical Criteria for Authentication

Philippe Colomban [1,*], Gulsu Simsek Franci [2] and Xavier Gallet [3]

[1] Sorbonne Université, CNRS, MONARIS UMR8233, Campus P. et M. Curie, 4 Place Jussieu, 75005 Paris, France
[2] Koç University Surface Science and Technology Center (KUYTAM), Office of Vice President for Research and Innovation, Koç University, Rumelifeneri Yolu, Sariyer, 34450 Istanbul, Türkiye; gusimsek@ku.edu.tr
[3] Musée National d'Histoire Naturelle, CNRS, Université Perpignan Via Domitia, Musée de l'Homme, UMR 7194—Histoire Naturelle de l'Homme Préhistorique (HNHP), 17 Place du Trocadéro, 75116 Paris, France; xavier.gallet@mnhn.fr
* Correspondence: philippe.colomban@sorbonne-universite.fr

Abstract: Nine glazed porcelain artifacts bearing the coat of arms of France, from King Louis XV tableware orders, were analysed at the laboratory or in their conservation secure room. Based on the experience acquired in the study of 18th century European and Chinese porcelain using mobile XRF (pXRF) and Raman microspectroscopy, a comparison of the impurities in the paste (Y, Rb, and Sr), the elements associated with cobalt in the blue overglaze (Bi, Mn, Zn, and As) and those present in the tin yellow and Naples yellow pigments (Sn, Sb, and Zn) highlights the use of different raw materials for some of these objects. Differences regarding the Ag content in the gold decorations also provide information. Raman identification of the different types of yellow pigment confirms the categorization. The results obtained on the Louis XV tableware are compared to those of "*Chine de commande*", attributed to the same places and periods of production or recognized copies. The clustering of the quantitative comparison pXRF signals of the abovementioned elements and a consideration of the Raman parameters of the yellow pigments appear to be effective tools for object categorization to confirm or refute questions about the authenticity of objects.

Keywords: porcelain; tableware; pXRF; Raman; Chine de commande; Louis XV; paste composition; impurities; blue; overglaze; cobalt; pyrochlore; yellow; gold; silver; provenance

Citation: Colomban, P.; Simsek Franci, G.; Gallet, X. Non-Invasive Mobile Raman and pXRF Analysis of Armorial Porcelain with the Coat of Arms of Louis XV and Others Enamelled in Canton: Analytical Criteria for Authentication. *Heritage* **2024**, *7*, 4881–4913. https://doi.org/10.3390/heritage7090231

Academic Editor: João Pedro Veiga

Received: 17 July 2024
Revised: 27 August 2024
Accepted: 29 August 2024
Published: 6 September 2024

1. Introduction

With the establishment of the Indian Companies, the *East India Company* (EIC), founded in England in 1600; the *Vereenigde Oostindische Compagnie* (VOC), founded in Holland in 1602; and the *Compagnie des Indes Orientales*, founded in France in 1664, the importation of Chinese and Japanese porcelain became important, particularly the production of emblazoned tableware services for the Courts and European elites [1–15]. These were enamelled in the workshops of the Customs district in Canton [16], with the porcelain bodies anticipated to have been made at Jingdezhen. These products made especially for export are called '*Chine de commande*'. Louis XV, King of France, ordered an important porcelain tableware service and other objects [17]. The centre of these objects is decorated with the coat of arms of France, which is azure with three golden *fleurs-de-lys*, the collar of the Order of the Holy Spirit, and the collar of the Order of Saint Michel, all under a closed royal crown. The polychrome decoration combines a blue underglaze decoration with blue, red, green, black, and gilding in an overglaze palette, and sometimes yellow and/or eggplant to grey colours. Consequently, these artifacts belong to *Famille verte* according to the 1862 classification of Albert Jacquemart [18]. Roughly, in the 1720–1730 period, Chinese export porcelain followed the *Famille verte* criteria (in the so-called Kangxi style), with

blue underglaze and 'transparent colour' overglaze. During the next decade, production followed the *Famille rose* criteria, characterized by the addition of new opaque overglazes. The order in question is attributed [17] to the development in 1738 of a new dining room on the second floor of the 'private' King's cabinets at Versailles castle. However, it is possible that the first order was made earlier, circa 1720–1722 (the years corresponding to the end of the reign of the Kangxi Emperor, the second emperor of the Qing Dynasty); other pieces were ordered up to the year 1740, i.e., during the reign of Emperor Qianlong. For instance, the order for twelve bidets with the coat of arms of France was placed with the *Compagnie des Indes Orientales* [17] in 1738. The order was made by the Directors of the French Company to the Board of Directors of Canton and was renewed due to the delay in manufacturing, and the whole set was eventually delivered in 1740. The details of the order are not known, but, traditionally, an 18th century tableware service amounted to between 112 and 122 pieces [17,19]. As the tableware was heavily used, it is likely that some pieces have been broken and replaced.

Objects decorated with the coat of arms of France attracted much attention from collectors in the 19th century and *Maison Samson* [20–22], who were known for creating pieces simulating the great masterpieces of ceramic art, and who produced similar objects in the last quarter of the 19th century and afterwards. These Qing porcelains continue to be sought after and are the subject of regular sales in major auction houses [23–31], including copies attributed explicitly to the *Samson* factory [32,33]. Experts distinguish 'authentic' objects from their copies by the comparative study of their dimensions, weight, paste colour, and decorations, and through the search for documents concerning them.

To our knowledge, there has been no analytical work on this type of royal porcelain apart from a preliminary study using Raman microspectroscopy by our group [34]. We present here the first combined study of non-invasive elemental analysis by portable X-ray fluorescence spectroscopy (pXRF) and the identification of crystalline and amorphous phases by Raman microspectroscopy of eight objects bearing the royal coat of arms of France (plus a comparison with previously published Raman data for another object) and six similar objects bearing other coats of arms of contemporary important personages. The objective is the research of analytical criteria for authentication. The availability of such objects being limited and their transport complicated, only certain pieces were analysed in the laboratory, while the others were analysed at their conservation site with mobile Raman and/or pXRF instruments. Furthermore, the access duration to the objects and, consequently, the number of measurements are limited. We will compare the results to those of other '*Chine de commande*' porcelain from the same period as well as to those of a '*Samson*' copy.

2. Materials and Methods

2.1. Objects

The objects from the Louis XV tableware service have been the subject of several studies, which should be referred to for a detailed description of the decoration and dating proposals [17]. The palette used red, blue, and gold colours, a type of decoration style called Imari due to its similarity with some Arita kiln porcelain (Kyushu, Japan). The objects and their most characteristic parts studied in this work are presented in Figures 1–10 and their main characteristics are listed in Tables 1 and 2.

Figure 1. Large dish (Private Collection); views of the analysed areas (see Table 1); (**a**) blue coat of arms and white areas on the central collar; (**b**) yellow area at the top of the basket and blue overglaze; (**c**) red flower and green overglaze; (**d**) red flower and green leaves (overglaze) on the back of the dish.

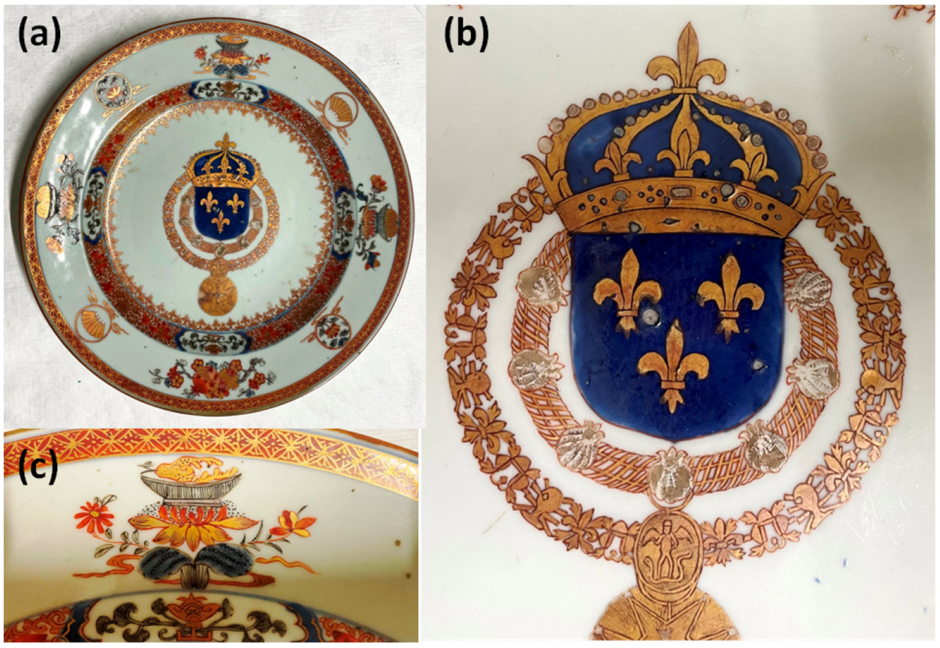

Figure 2. Plate (Musée du Petit Palais Collection); views of the analysed areas (see Table 1): (**a**) full view; (**b**) blue coat of arms and the central collar; (**c**) note the lack of yellow area at the top of the basket with red, blue and green overglazes.

Figure 3. Mustard pot (Private Collection; (**a**,**b**) views of the two sides); analysed areas are the blue coat of arms, the white areas on central collar and the different overglaze with the basket; (**c**) small tureen, see ref. [34] (Private Collection).

Figure 4. Tureen (Private Collection); views of the analysed areas (see Table 1): (**a**) blue underglaze coat of arms and blue, white, red and green overglaze (**b**–**d**); note the white dots in relief on the central collar and the crown basement and the lack of yellow at the top of the basket.

Figure 5. Knife handles ((**a**) 28710A; (**a'**) 28710B) and torch ((**b**) 12292) (Musée des arts décoratifs Collection). The green laser spot shows analysed area of the blue overglaze. The analysed areas are listed in Table 1.

Figure 6. Ewer (**a**); (**b**,**c**): views of the analysed areas: blue, red, green, white and yellow areas (see Table 1); Rothschild10, Musée des arts décoratifs Collection.

Figure 7. Tureen decorated with Philibert Orry coat of arms (Priv. Coll.): (**a**) view, (**b**–**d**) zooming on different overglazes, and (**e**) view of the object setting during Raman analysis. See Table 2 for analysed areas.

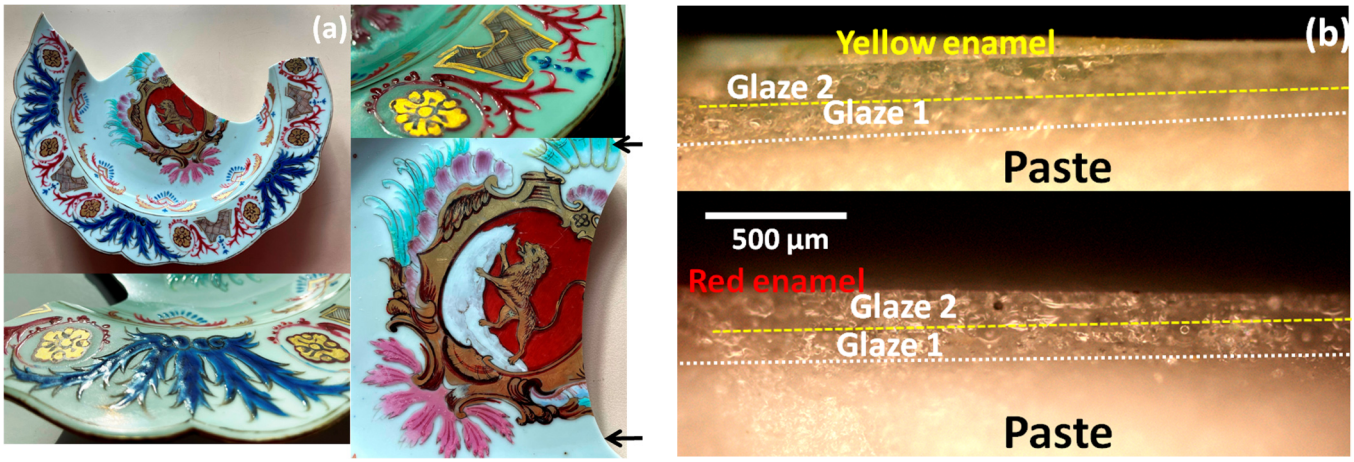

Figure 8. Broken plate decorated with Philibert Orry coat of arms (Private. Coll.); (**a**) surface and (**b**) section view; arrows indicate the section view (note the different layers; knowledge of typical glaze and overglaze thicknesses is important in evaluating pXRF data); dashed lines are guides for eyes delimiting the different layers. See Table 2 for analysed areas.

MAD SN27A MAD SN27B *Samson?*

Figure 9. Two plates with Elias Guillot coat of arms (SN27A and SN27B) with detailed view and a plate with unidentified coat of arms attributed to *Samson* factory (Musée des arts décoratifs Collection). See Table 2 for analysed areas.

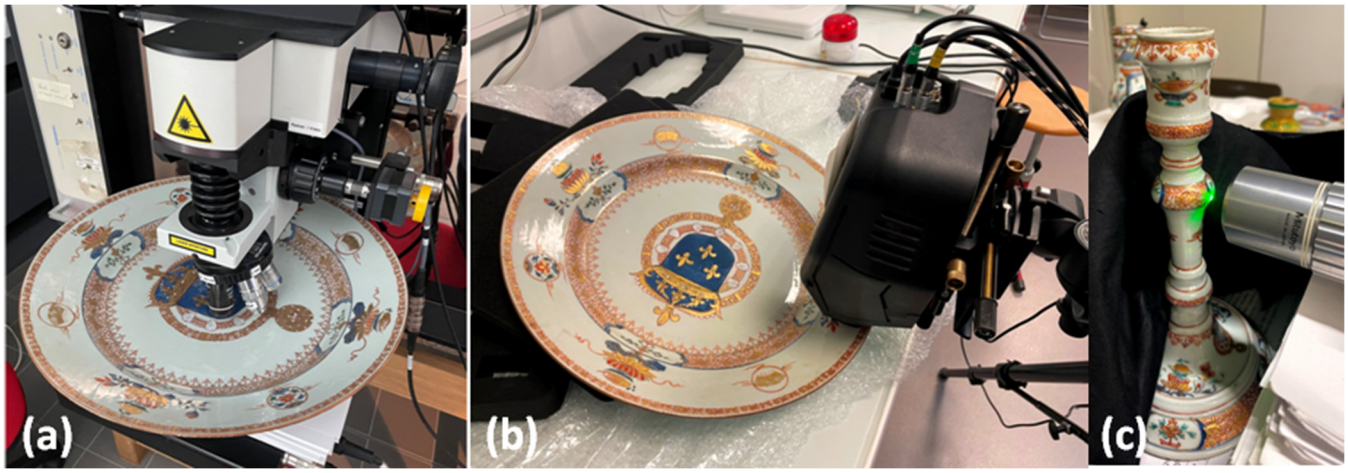

Figure 10. Examination of artefact at the laboratory (**a**) width bench-top Raman spectrometer, (**b**) mobile XRF and (**c**) mobile Raman spectrometer.

The enamelled decoration of these objects shows some differences from a simple visual examination. Some have small yellow areas of overglaze enamels (large dish (Figure 1b), mustard pot (Figure 3a), and objects of the *Musée des arts décoratifs* (MAD), Figure 6), while these colours are absent from the decoration or from certain parts of the decoration of other pieces (replaced with some pale grey or eggplant colour, e.g., the plate belonging to the *Musée du Petit Palais* (MPP); Figure 2c). On some pieces, different shades of red are evident. The opaque white highlights are only visible on some of the pieces. From these different visual criteria, doubts exist about the authenticity of the plate (MPP Coll.) and the large tureen (Priv. Coll.). A small tureen with the same decoration has already been studied using Raman microspectroscopy [34], and the results will be compared.

Around the collars (Figures 1a, 2b, 3b and 4a) surrounding the coat of arms are four cartridges containing the "L" monogram of King Louis XV in green foliage (Figure 1b). Red flowers and green foliage are on the reverse of the large dish (Figure 1d). On the marli, a decorative motif represents an underglaze blue lotus leaf (Figures 1c and 4c), on which rests a chrysanthemum flower, itself supporting a basket with a lemon. In some objects, the top of the basket is filled in with a pale yellow (e.g., Figures 1b and 5a'). The expected dates of production are given in Table 1, the first set being from a ca. 1722 order and the other from the ca. 1738 to 1743 order.

Three dishes with the same decoration as the large dish and the plate (but in a different format) are on show at the *Château de Versailles*, and another large dish is at the *musée de la Compagnie des Indes* located in Port Louis/Lorient [13]. Certain objects with these French arms, which are likely to belong to the orders of Louis XV, have been the subject of recent sales [22–31]. Some of these objects have, however, been attributed to the *Maison Samson* [32,33].

Table 1. Artifacts decorated with the French royal coats-of-arms (MAD: Musée des arts décoratifs, Paris; Priv.: Private collection; MPP: Musée du Petit-Palais, Paris; n. a.: not analysed, *ca.*: circa). Specific colours are in bold. Assumed or known periods are given in italics.

Name ***Period***		**Collection/ Inventory Number**	**Colours/Areas Analysed in pXRF**	**Colours/Areas Analysed in Raman**	**Figure [Ref.]**
Large dish *ca. 1722?*		Priv. Coll.	body, glaze, blue, white, red, **yellow, green**, gilding	blue, white, red, black, brown **yellow, green**,	Figure 1
Plate ?		MPP	body, glaze, blue, white, red, gilding	n. a.	Figure 2
Mustard pot *1725/1728?*		Priv. Coll.	body, glaze blue, white, red **yellow, green** gilding	n. a.	Figure 3a,b
Ewer *ca. 1725/1735*		MAD Rotschild10	n. a.	blue, white, red black, pink, brown **yellow, green**	Figure 6
Tureen (small) *ca. 1725–1728*		Priv. Coll.	n. a.	blue, white, red black **green**	Figure 3c [34]

Table 1. *Cont.*

Name *Period*		**Collection/ Inventory Number**	**Colours/Areas Analysed in pXRF**	**Colours/Areas Analysed in Raman**	**Figure [Ref.]**
Tureen (large) Bottom & Lid *?*		Priv. Coll.	body, glaze blue, white, red **green**, gilding	blue, white, red purple, black	Figure 4
Knife handle *ca. 1739/1740*		MAD 28710A	n. a.	glaze blue, red black **yellow, green**	Figure 5a
Knife handle *ca. 1739/1740*		MAD 28710B	n. a.	blue **yellow, green**	Figure 5b
Torch *ca. 1739/1740*		MAD 12292	n. a.	blue, red black **yellow, green**	Figure 5c

The objects of comparison (Table 2) consist of two objects ordered by Philibert Orry, ca. 1730 [35–38], a soup tureen and a dish, already partly studied [34], and four plates, three of them bearing the arms of Ellias Guillot (1695–1743), Governor of the Coromandel Coast (1733), Consul Extraordinary of India and Director General of India (1742) [39], assigned to ca. 1740–1743, and the other with an unidentified coat of arms. This last plate is considered to be a 19th/20th century production, possibly by the *Samson* factory, which was active from ~1849 to 1992, mainly in Montreuil, a city near Paris [20–22]. One of these artifacts has already been partly studied [40].

Table 2. Artifacts for comparison (MAD: Musée des arts décoratifs, Paris; AR: Musée de l'Ariana, Genève; n. a.: not analysed). Assumed or known periods are given in italics.

Name [Period]		**Collection/ Inventory Number**	**Colours/Areas Analysed in pXRF**	**Colours/Areas Analysed in Raman**	**Previous Study [Ref.]**
Philibert Orry' tureen *ca. 1730*		Priv. Coll.	n. a.	blue, white, red green, sea green orange	

Table 2. *Cont.*

Name [Period]		Collection/ Inventory Number	Colours/Areas Analysed in pXRF	Colours/Areas Analysed in Raman	Previous Study [Ref.]
Philibert Orry' plate ° *ca. 1730*		Priv. Coll.	n. a.	body, glaze blue, white, red pink yellow, turquoise	
Elias Guillot' plate *ca. 1740/1743*		MAD SN27A	n. a.	blue, red brown	
Elias Guillot' plate *ca. 1740/1743*		MAD SN27B	n. a.	blue	
Elias Guillot' plate *ca. 1740/1743*		AR 3680	glaze blue	n. a.	[40]
X plate (*Samson 1920?*)		MAD		glaze blue, red black yellow, green	

° The availability of this broken object allows us to know the thickness of the glaze (~300 to 400 µm) and overglazes (~50 to 250 µm) for large areas, and up to 500 µm for over-thickness enamels (see further).

Philibert Orry was *Contrôleur général des finances* and *Directeur général des Bâtiments* for King Louis XV [37,38]. His half-brother, Jean-Louis Henry Orry, was the *Directeur de la Compagnie des Indes* [38] and one of the founders of the Vincennes porcelain factory, which was then made over to Louis XV and moved to Sèvres city [41].

2.2. Techniques

Measurement set ups are shown in Figure 10.

2.2.1. Portable X-ray Fluorescence Spectroscopy (pXRF)

The procedure is described in detail in a previous article [40]. X-ray fluorescence analysis was performed on site using a portable instrument (Elio, Milano, Italy). The set-up included a miniature X-ray tube system with a Rh anode, a ~1 mm^2 collimator, and a large-area Silicon Drift Detector with an energy resolution of <140 eV for Mn Kα, with an energy range of detection from 1.3 keV (in air) to 43 keV. The working distance between the instrument front and the analysed spot is 1.4 cm, which permits the selection of coloured areas located on flat or rather convex zones, but the shape of the instrument front often imposes a working distance

of ~0.5 cm. Depending on the object, the measurement was carried out by positioning the instrument on the top or on the side. Perfect perpendicularity to the area measured is desirable. Measurements were carried out in the point mode with an acquisition time of 180 s, using a tube voltage of 50 kV and a current of 80 μA. No filter was used between the X-ray tube and the sample. The analysis depth during the measurement of the enamel was estimated from the Beer–Lambert law (the analysis depth is here defined as the thickness of the top layer from which comes 90% of the fluorescence) [42] to be close to 6 μm at Si Kα, 170 μm at Cu Kα, 300 μm at Au Lα, and 3 mm at Sn Kα. These values should be compared with the thicknesses of the overglazes, which range from ~50 to 500 μm.

The accuracy of the instrument is controlled by measuring reference glass and stone samples [43]. The data fitting procedure with Artax 7.4.0.0 (Bruker, AXS GmbH, Karlsruhe, Germany) software is described in previous papers [40,43]. The net area was calculated under the peak at the characteristic energy of each element selected in the periodic table, and the counts of the major, minor, and trace elements were determined in the coloured areas (white, red, yellow, orange, blue, green, and black). Before plotting the diagrams, the net areas of each element were normalized by the number of XRF photons derived from the elastic peak of the X-ray tube of rhodium. Normalization with respect to the signal of Co was made for the comparison of blue-containing elements for artefacts prepared with very different technologies at different times. Then, these normalized data were plotted in the ternary scattering diagrams. Additionally, Euclidian hierarchical similarity plots were drawn for the interpretation and discussion of the results with Python software (version 3.12.4). The procedure used results from experience acquired in the analysis of hundreds of objects. The intensities of the peaks of the electronic transitions (Kα, Kβ, Mα, Mβ, Lα, Lβ, Lγ, etc.) giving the characteristic peaks depend firstly on the elements concerned and secondly on the contents of these elements. This is why, for example, the peak of the major element Si (silicon) can be smaller than minor elements (Pb contamination) and comparable to that of Rb traces. In addition, a complex-coloured decoration requires a topological variation in the three dimensions of the colouring agent concentration. The raw intensities, therefore, have no meaning, and this is why we developed the clustering analysis procedure in different diagrams comparing the areas of characteristic peaks. The access time to the objects was limited; consequently, only one or sometimes two measurements were made. Previous work [43] showed that the variability of results for equivalent-coloured areas did not affect the conclusions in the clustering analysis procedure based on the comparison of peak areas.

2.2.2. Raman Microspectroscopy

As in our previous studies (see reference [34] and references herein), artefacts were analysed in the laboratory using a Labram HR800 spectrometer (HORIBA Scientific Jobin-Yvon, France) excited by an Ar^+ ion plasma laser Innova I90C 6UV (Coherent Inc., Santa Clara, CA, USA) and some others on site using a mobile HE532 set up (HORIBA Scientific Jobin-Yvon, Palaiseau, France) equipped with Ventus YAG laser (Laser Quantum, Fremont, CA, USA). The availability of objects being limited, the analysis conditions vary depending on the objects being studied.

The 457.9 and 514.5 nm lines of Ar^+ laser were used at the laboratory with approximately 0.5 (dark-coloured enamels) to 10 mW (paste, glaze and light-coloured enamels) power of illumination at the sample surface for the blue line and 0.2 to 2 mW for the green line. Long working distance (LWD) 50× and 100× microscope objectives (Olympus Corp., Tokyo, Japan) were used. Analysed spots are about 5 × 5 and 2 × 2 μm^2; the in-depth penetration is similar for the colourless glaze, respectively, and strongly reduced for dark-coloured areas. Typically, 50–4000 cm^{-1} spectral window was studied. Counting time ranged between one minute or less and a few tenths of minutes (at least 3 accumulations to suppress cosmic ray signals). Systematically, three spots are analysed per area considered.

The power of illumination used with the mobile 532 nm set-up (YAG laser) ranges between 2 (dark-coloured areas) and 20 mW (light-coloured areas). Long working distance

(LWD) 50× (Nikon Corp., Tokyo, Japan) and 200× (Mitutoyo, Kanagawa, Japan) microscope objectives were used. The spectral window ranges from 50 to 3200 cm^{-1}. Counting times are less than a few minutes per spectrum with a minimum of 3 to 30 accumulations. The measurement campaigns were carried out in different conditions (room temperature), and the limited resolution of the instrument led to an uncertainty of ±2 cm^{-1} on the wavenumbers. The procedures are defined on the basis of experience acquired over 20 years in the analysis of hundreds of objects.

3. Results

We will first compare the pXRF spectra obtained on the different surface areas constituting the porcelains (unglazed body, glaze and coloured overglaze, gilding). Then, we will compare the areas of the characteristic XRF peaks of the elements. This method makes it possible to categorize the pastes and glazes prepared with the same raw materials [40]. Then, the Raman spectra will be used to identify the opacifier and pigments before discussing the enamelling technique of each artefact to discuss their period of production and provenance/authenticity.

3.1. Paste and Colourless Glazes

A comparison of the pXRF spectra of the pastes and the transparent glazes (Figure 11) highlights small differences concerning the contamination by lead induced on the surface of the paste during the firing of the lead-based enamels (virtually no contamination is observed for the large tureen, indicating different firing conditions, but a small Pb contamination is observed for the lid) as well as differences in the K/Ca, Rb/Sr, and Rb/Pb ratios (Figure 12). The Pb contamination arises from the high volatility and reactivity of PbO above 800 °C.

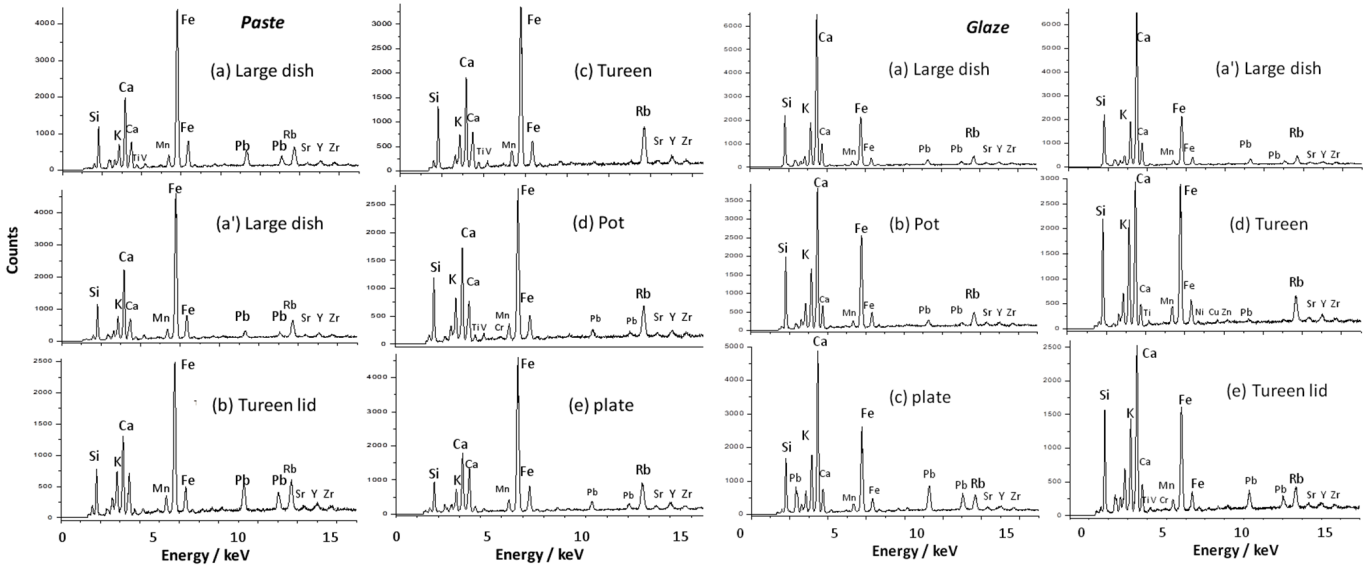

Figure 11. pXRF spectra of paste (**left**) and glaze (**right**) of porcelains decorated with coat of arms of France (see Table 1).

For the colourless glazes, we note visible variations concerning the peak intensities of K and Ca elements as well as Mn, Fe, and V. The composition of the large tureen (bottom part) glaze shows a higher K/Ca ratio. Examination of the ternary diagrams constructed from the peak area variations confirms the two groups (here after called G_{Ca}:K/Ca < 1.7 and G_K:K /Ca~ > 1.7).

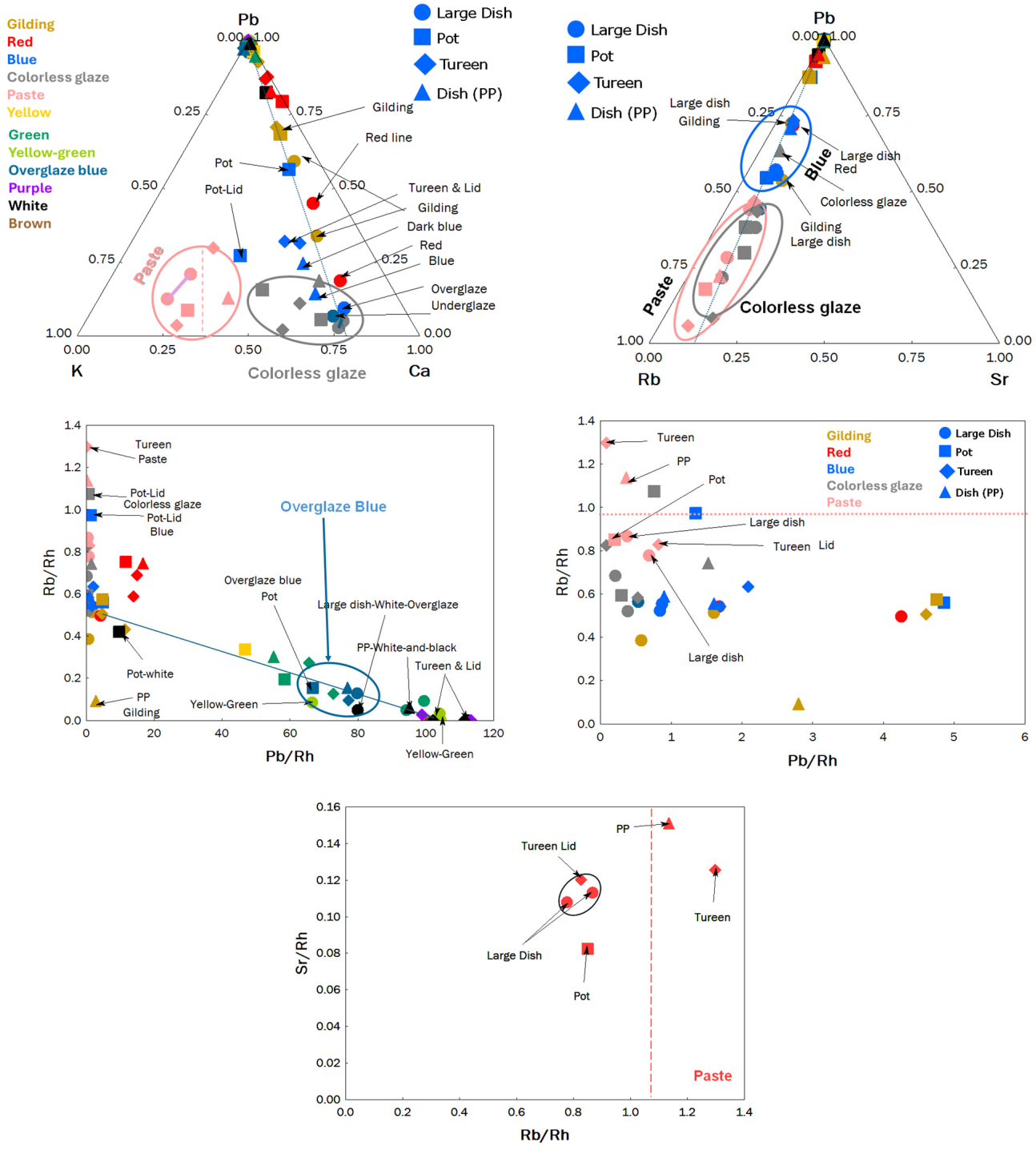

Figure 12. Peak intensity Pb-K-Ca and Pb-Rb-Sr ternary diagrams, Rb vs. Pb biplot (full scale and zoom) and Sr vs. Rb biplot of data related to the paste. Lines are guides for eyes.

The distribution of intensities for the overglazes along a straight line from the vertex Pb towards the area of the measurement values for the colourless glazes results from the variation in the thickness of the overglaze, a thickness less than the depth at which the detection of lead is made (a few hundreds of μm). The differences in the K/Ca ratio between the paste (richer in potassium) and the glaze (richer in calcium) are obvious (Figure 12).

Differences between the two measurements made on the large dish illustrate the variability of the measurements (there is an intrinsic heterogeneity of the material—paste and glaze—and errors due to variable glaze thickness, as usual for pXRF analyses [43]).

We observe the largest difference between the measurement concerning the body and the lid of the large tureen. The Rb/Pb biplot and, in particular, the zoom on the low values concerning the body (without or contaminated by lead during the firing of enamelled decoration) and glaze highlight two types of paste, the large dish, the mustard pot and the lid of the tureen on one side and the PP plate and the bottom of the tureen on the other side. This indicates the use of different raw materials providing calcium, sodium, and potassium for each group. The Sr vs. Rb biplot, i.e., the comparison of the signal of these impurities provided by the material leading to fusion (flux), confirms two or three groups: PP plate and tureen bottom on the one hand and tureen lid, large dish, and mustard pot on the other hand, although the latter is a bit apart. It is clear that we have two or even three different productions made using different raw materials, corresponding to different periods and/or places of production.

3.2. Underglaze and Overglaze Blue

Figure 13 compares the pXRF spectra recorded on the blue underglaze areas. The drawing of the blue colour being applied under the glaze means that the contribution of the glaze will be significant. It is appropriate to only consider the peaks whose intensity is stronger than in the colourless glaze (Figure 11). This is obviously the case for the elements Mn and Co (the Kα peak of cobalt is on the right side of the Kβ peak of iron). The Kα contribution of cobalt is seen by the broadening of the peak, and the Kβ one is on the right side of the Ni peak. As for paste surface, contamination by lead on the glaze surface is variable. The spectra of the large dish and the PP plate are close (CoU1 group), different from those of the mustard pot and the large tureen (CoU2 group).

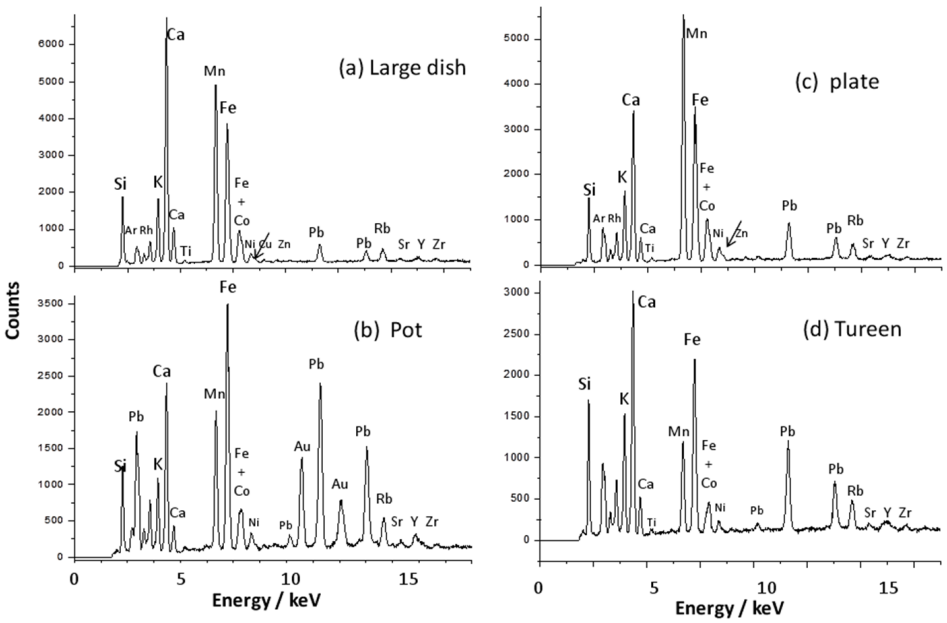

Figure 13. Blue underglaze pXRF spectra of porcelains decorated with coat of arms of France. Arrow indicates the broadening of the Fe Kβ-Co Kα double peak (see Table 1).

The spectra for overglaze blue are very distinct (Figure 14). These spectra are dominated by the M (low-energy range) and L (medium-energy range) transition peaks of lead. Zooming in on the peaks of other elements allows for detailed comparisons. Significant differences also involve transition metals and elements geologically associated with cobalt, such as Mn, Fe, Ni, Cu, Zn, and As, as well as the K/Ca ratios [44,45].

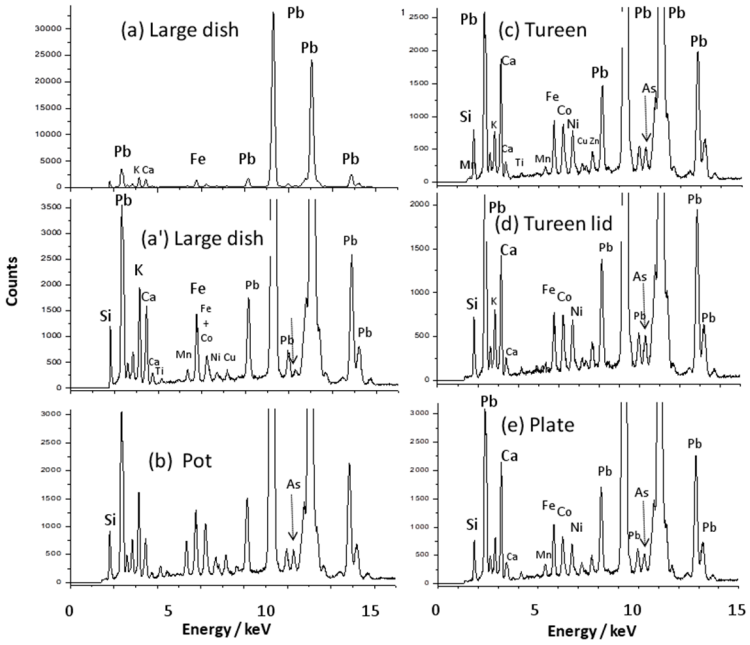

Figure 14. Blue overglaze pXRF spectra of porcelains decorated with coat of arms of France (see Table 1).

The spectra obtained on the blue overglazes of the large tureen, and its lid, differ significantly regarding the Mn signal. Excluding the contribution of Fe and the associated Mn in the colourless glaze under the overglaze, the cobalt used for the large dish, the PP plate, and large tureen is almost free of manganese, rich in arsenic, and contains nickel, zinc, and traces of copper. This signature is typical of cobalt imported from Europe [34,40,45–49]. The pot spectrum shows a higher level of manganese, too high to be unrelated to cobalt. This indicates the use of (likely less expensive) cobalt traditionally used under the Ming Dynasty and the beginning of the reign of Kangxi mixed with imported European cobalt, a technique observed during the reign of Qianlong for Canton productions [40].

Figure 15 visualizes the different types of cobalt used for underglaze blue and overglaze blue, as widely demonstrated for Qing porcelains [34,40,45–48]. Note the lower Mn content of blue overglaze of the tureen (bottom) and the PP plate.

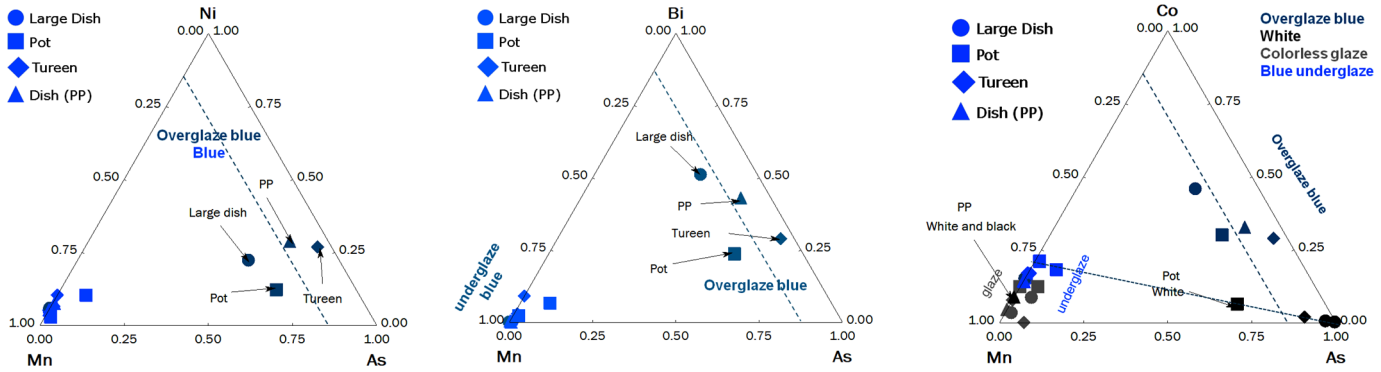

Figure 15. Co-Mn-As, Bi-Mn-As and Ni-Mn-As diagrams for measurement of blue (over- and under-glazed blue) and white (opaque and transparent) areas. Dashed lines are guides for eyes.

3.3. White Painted Overglaze

Opaque white enamel dots are visible on the collar surrounding the coat of arms and in certain places on other pieces (e.g., the flower petals of ewer decoration, Figure 6). Figure 16 compares the XRF spectra recorded for the large dish, the mustard pot, the large tureen,

and the PP plate. The presence of arsenic—arsenates of lead, calcium, and potassium, the classic opacifiers of Qing enamels [34,40,45,46]—is clear for the large dish and the large tureen (see Figure 15). Although gold significantly contributes to the spectrum of the gilded areas of the mustard pot, we can exclude the presence of arsenic in its decor, and the peak ratio of the Au peaks is as expected. No arsenic is found for the plate. Therefore, we have two different types of enamelled decoration. Surprisingly, a rather high level of zinc is observed in the large dish, and as traces in pot and tureen (bottom), but not detected in the plate and the tureen lid.

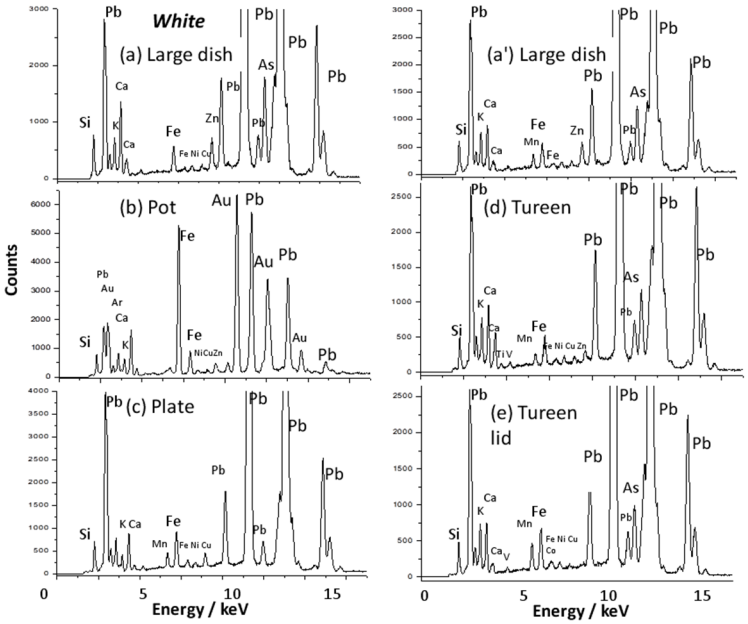

Figure 16. pXRF spectra of white (overpainted) areas of porcelains decorated with coat of arms of France.

3.4. Yellow and Green

Figure 17 compares the spectra of yellow and green enamelled areas. As expected, the large dish and mustard pot show that green colouration is achieved by Cu^{2+} ions, while yellows are based on lead–tin yellow. Further analysis of these pigments will be discussed using their Raman spectra. Variability is observed in the spectra obtained from different spots, with traces of nickel and zinc detected in the yellow overglaze.

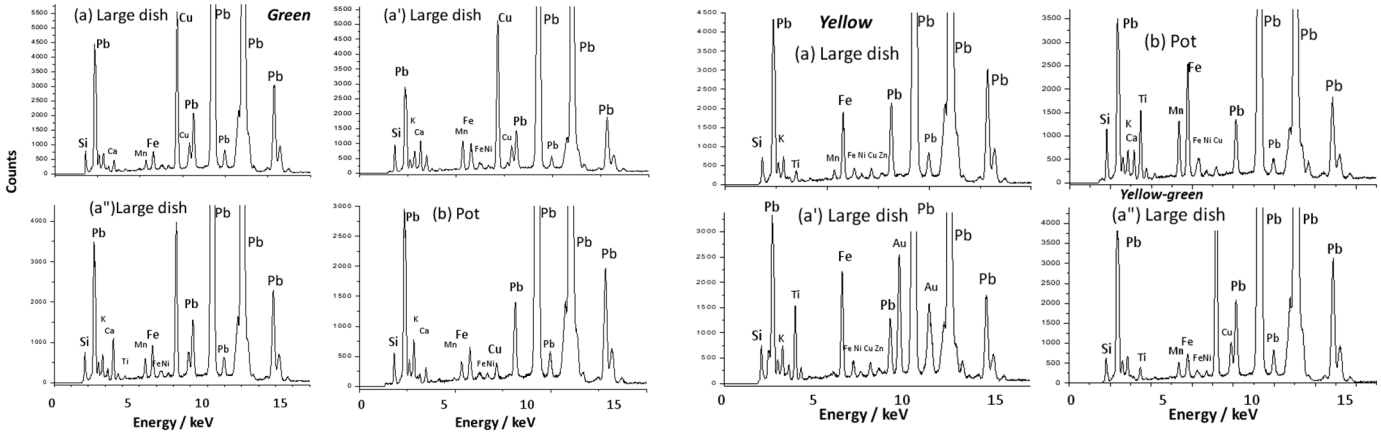

Figure 17. Yellow (**right**) and green (**left**) overglaze pXRF spectra of porcelains decorated with coat of arms of France: (**a**–**a"**), large dish; (**b**) mustard pot (see Table 1).

Figure 18 presents a comparison of the relative peak areas of the main elements stabilizing the pyrochlore phase of Naples Yellow-tin, antimony, and zinc, as well as characteristic impurities in the raw materials (Sr, Y, and Rb) (see [50] and references cited therein). Visual examination of the artefacts indicates the rarity or challenges associated with implementing this colour due to the scarcity of areas coloured in yellow. Lead–tin yellow emerged towards the end of the Ming Dynasty (Wanli reign, 1582–1620), coinciding with its introduction in Japan (Arita kilns) by Portuguese missionaries [51], but its use remained limited. There is a notable variability in the zinc signal for the large dish, yet a relatively consistent Sn/Sb ratio is maintained (Figure 18). Clear differences in composition are evident between the lid (a Pb-Sn-Sb mixture with minimal zinc) and the bottom of the large tureen (no Sb), confirming observations regarding the Rb signal of the body.

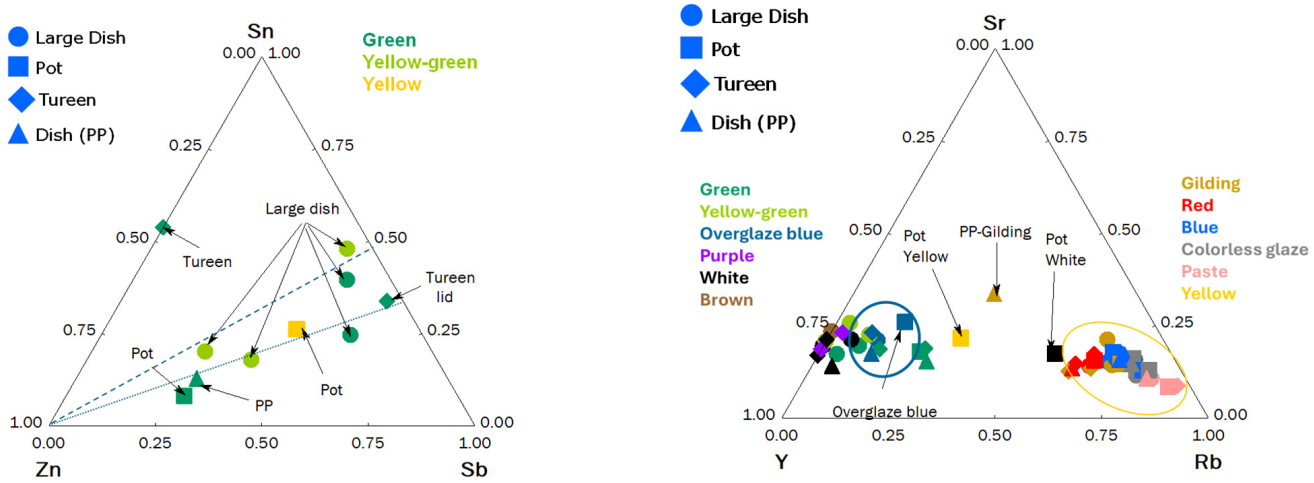

Figure 18. Peak area related ternary diagrams of Sn, Zn and Sb elements (**left**) and characteristic impurities (Sr, Y and Rb, **right**).

3.5. Red and Pink

The decor features areas ranging in colour from deep red to pink or brown hues. In certain instances, such as the mustard pot, large dish, large tureen, and PP plate, the red hues derive from iron red (Figure 19). Traces of gold detected in the mustard pot and small plate suggest the use of gold nanoparticles for colouring, a technique imported from Europe [34,46], giving rise to what is known as *Famille rose*. However, gilded decorations associated with red tones, like those seen in Figure 1c, can complicate spectral analysis by blending signals derived from adjacent red areas. For example, the high intensity of gold peaks in one of the red areas of the large dish (the necklace) stems from neighbouring gilding. The decoration of the pot, therefore, appears different from that of the other objects. The signal of gold derived from the nanoparticles present in purple to red areas (e.g., Figure 19d) is always very low due to the small amounts of gold required to obtain a vivid red to purple colour (expected of 0.1 to 1% wt Au°). Moreover, the narrow width of the red lines and their thin application mean that measurements (bearing in mind the pXRF spot diameter of approximately 1 mm^2) are heavily "influenced" by the underlying and neighbouring glazes. This complicates comparisons, necessitating a focus on differences significant enough to distinguish from glaze measurements.

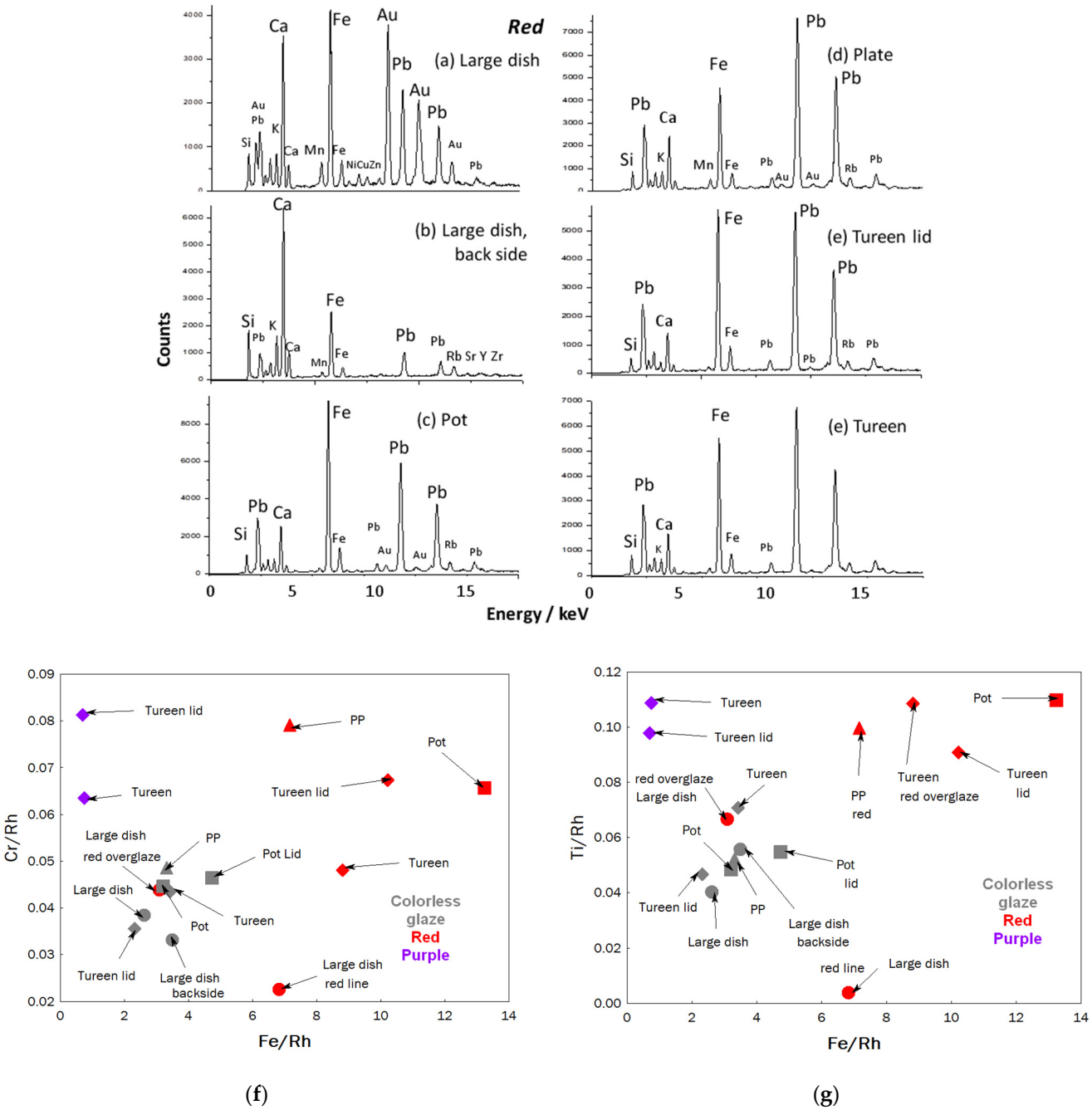

Figure 19. pXRF spectra of red overpainted areas of porcelains decorated with coat of arms of France ((**a**), main face and (**b**), backside: large dish; (**c**): mustard pot; (**d**): plate; (**e**): tureen lid and bottom) and comparison of Cr (**f**) and Ti (**g**) vs. Fe signal (shown with different symbols: circle for Large dish, square for Pot, triangle for PP, and lozenge for Tureen).

3.6. Gold

Figure 20 compares the peak areas of characteristic gold and silver peaks, revealing varying levels of silver addition across all objects, a common observation [52]. A notably high level of Fe in one measurement likely originates from the substrate. The distinctive purple colour seen in the large tureen is achieved using gold nanoparticles, precipitated through the addition of tin following the Kunckel method [53–56]. Contrary to techniques observed in other Chinese enamelled porcelain [56–60], the Perrot method involving arsenic is not detected. Traces of manganese are likely impurities already present in the glaze matrix.

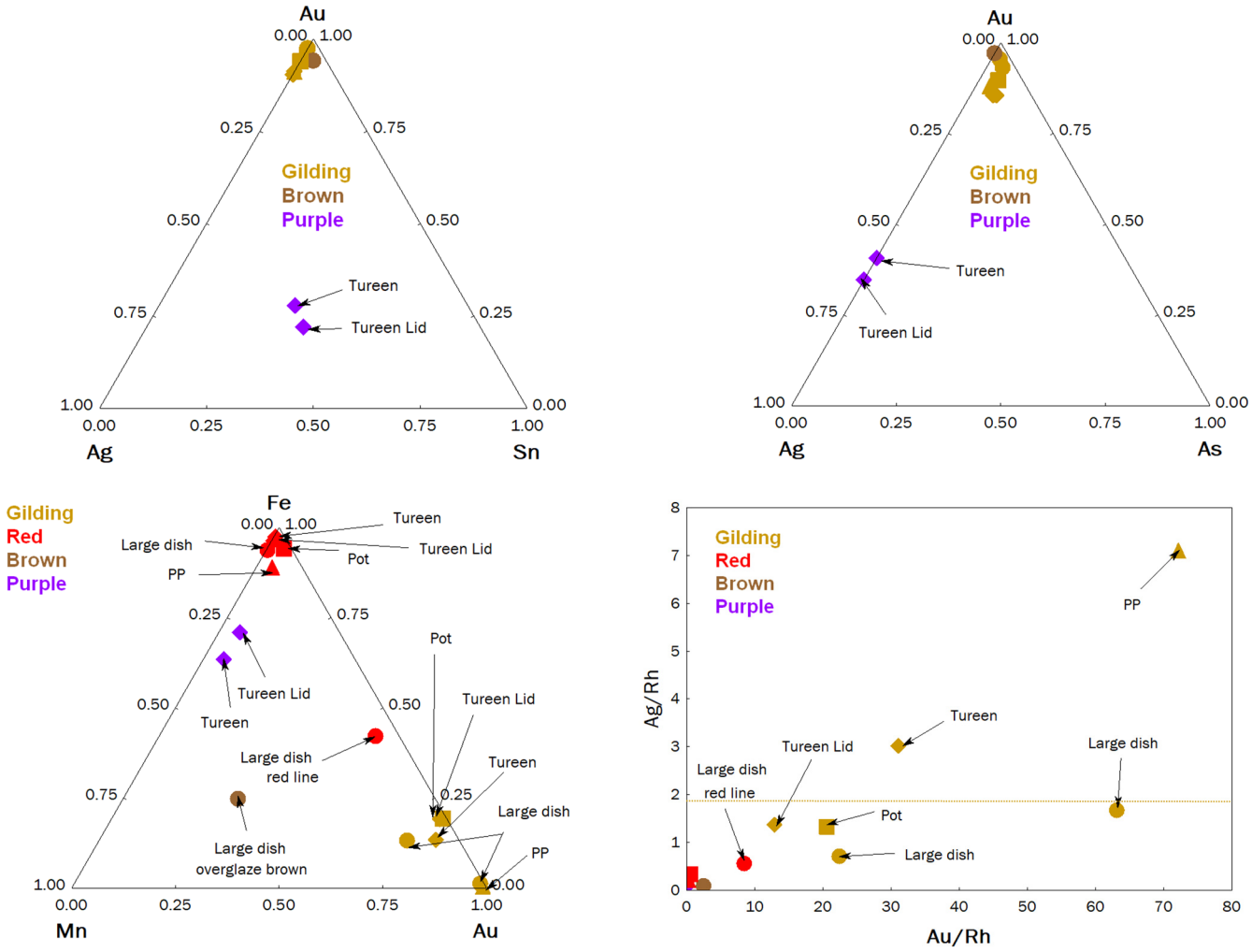

Figure 20. Peak area related ternary diagrams of Au and associated elements (Ag, Sn, As, Mn, Fe) and Ag vs. Au biplot (normalized with Rh signal) for gilded, red, brown and purple areas of the studied porcelains (shown with different symbols: circle for large dish, square for pot, triangle for PP, and lozenge for Tureen) (see Table 1).

Comparative analysis of silver and gold signals clearly indicates differences between the lower part of the tureen and the PP plate compared to other objects, highlighting that the gilding on the lid of the tureen differs from that on its lower part.

3.7. Phase Identification

Raman spectroscopy, a non-invasive analytical method, effectively identifies crystalline phases, opacifiers, pigments, and residual raw materials within artefacts that have not fully transformed, as well as the types of vitreous matrices. Figures 21 and 22 compare the Raman spectra of the two identified 'groups' by pXRF: the 'standard' group (including the large dish, torch, knife handles, and ewer) and a piece from the 'second' group (bottom of the large tureen). Initially, similar Raman signatures are recorded across all artefacts, resembling those previously documented for Canton productions [34]. We will consider each coloured area in detail to reveal the small differences.

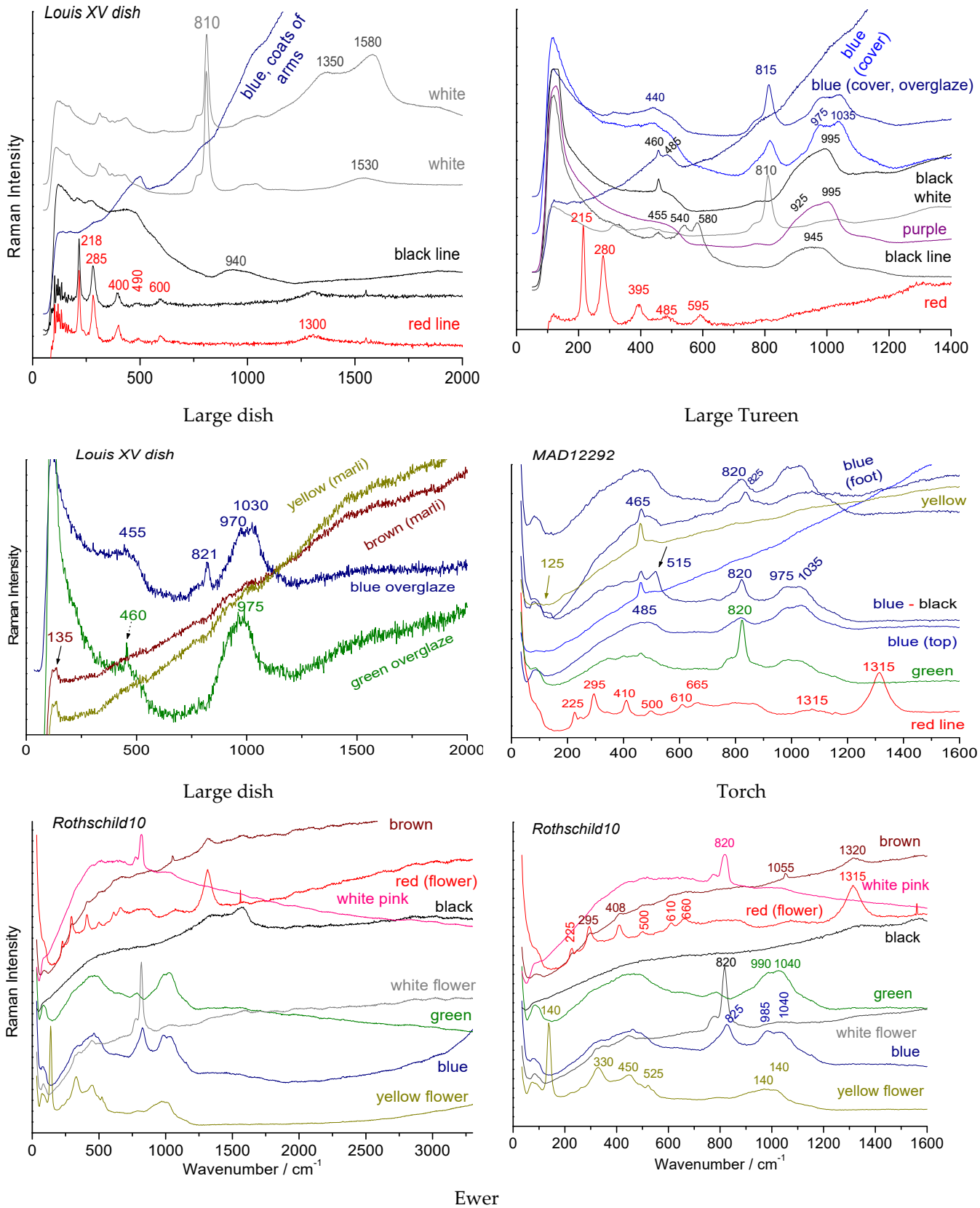

Figure 21. Representative Raman spectra recorded on large dish, large tureen (at the laboratory under 457.5 nm laser excitation and HR800 spectrometer) and on torch (MAD 12292) and ewer (MAD Rotschild10) with 532 nm exciting laser line (on-site analyses).

3.7.1. Blue Under- and Overglaze

Differences observed in the pXRF data are confirmed by Raman microspectroscopy. In blue-coloured underglaze and colourless (appearing white) areas, Raman spectra exhibit weak signals with strong and broad fluorescence (continuous background increase). The broad band around 480 cm^{-1} is characteristic of a high-melting aluminosilicate glassy phase [34,56,60] (seen in the large dish, large tureen, 12292 torch, Figure 20; 28710A and 28710B knife handle Figure 21; Orry plate, Figure 22). Occasionally, a narrow peak around ~465 cm^{-1} corresponding to quartz deformation mode is discernible [61]. Rutile traces are detected in the blue of 28710A, evidenced by a broad doublet around ~440 and 610 cm^{-1}.

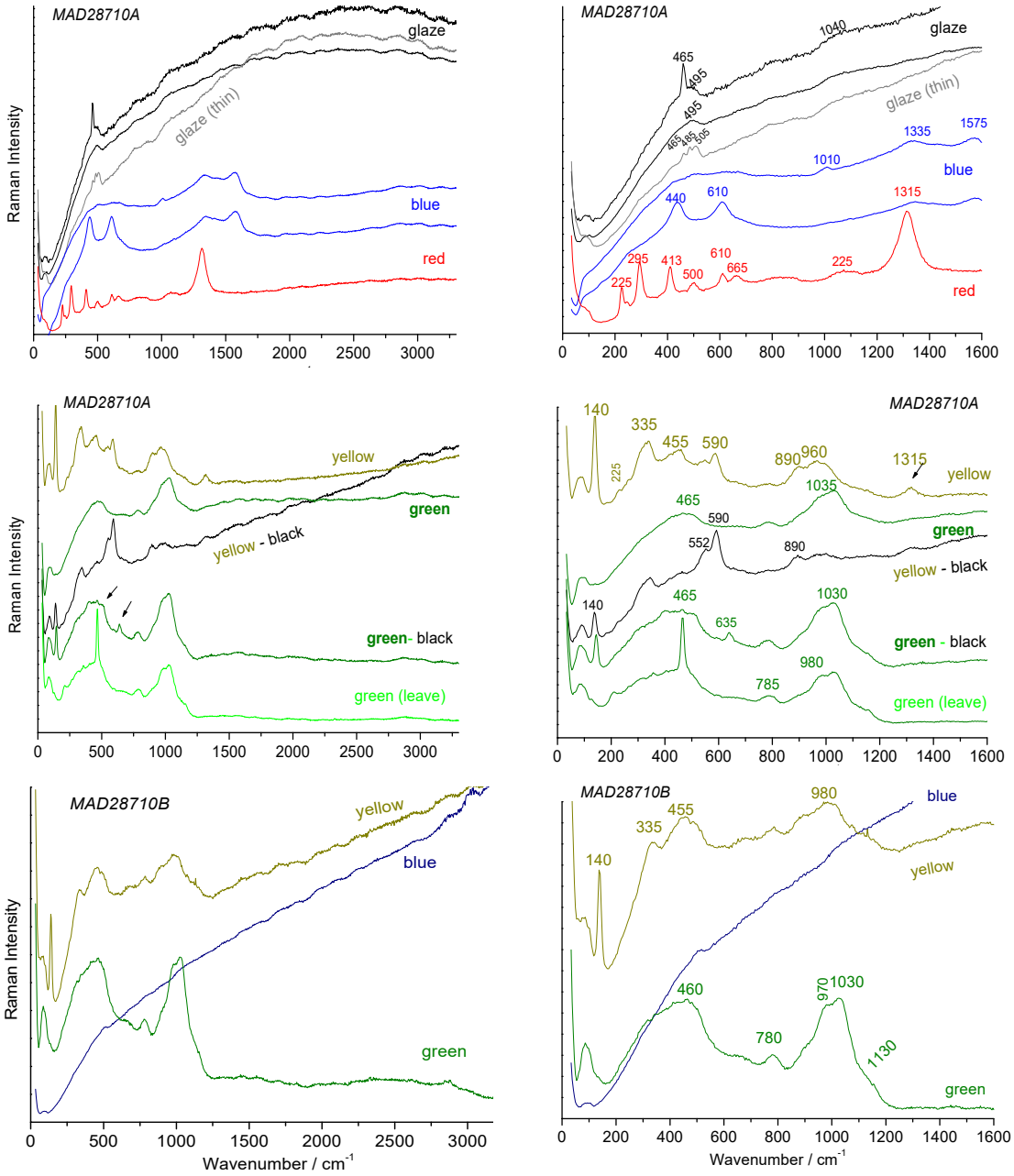

Figure 22. Representative Raman spectra recorded on knife handles (MAD 28710A and 28710B) with 532 nm exciting laser line (on-site analyses).

Conversely, blue overglaze spectra feature a prominent peak around 815 cm^{-1} (Figure 23), characteristic of the As-O stretching mode in lead calcium/potassium arsenate [46,62,63].

Different variations in the width of peaks (indicative of structural disorder) and their wavenumber positions are observed. A broader peak suggests a disordered structure, which can be intrinsic or influenced by the nano size of crystals present. These variations in spectral parameters undoubtedly depend on the specific phase formed and its composition [62].

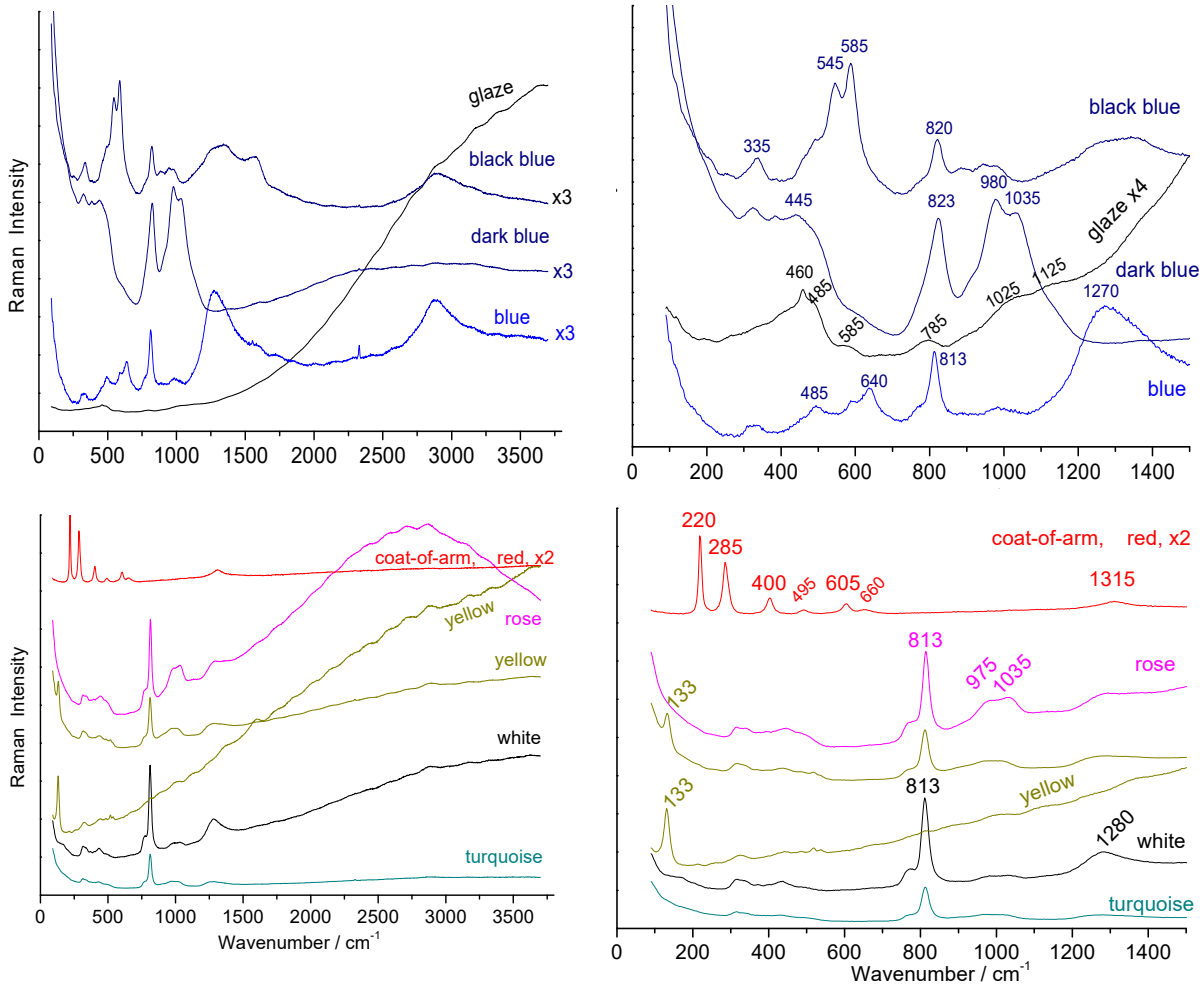

Figure 23. Representative Raman spectra recorded on Orry' plate with 457.5 nm exciting laser line and HR800 spectrometer.

The spectral signature of the silicate matrix in the blue overglaze exhibits a broad stretching mode band of the SiO_4 vibrational unit, with main components around 970–980 and 1035 cm^{-1}, characteristic of alkaline–lead glass [64], similar to Iznik fritwares [65]. This signature is consistently observed in the large dish, large tureen, torch, ewer and plates SN27A and SN27B.

In contrast, the plate attributed to Samson (Figure 24) shows a distinctly different signature in its light-blue overglaze, featuring a doublet at 635–775 cm^{-1} characteristic of cassiterite, along with broad features around 850 and 1000 cm^{-1}. Cassiterite was historically used only for light-green colours during the Qing Dynasty, primarily in exceptional imperial pieces influenced by the Jesuit guidance [40,66–68]. The presence of cassiterite in the blue area of the Samson plate suggests its European origin. However, a small amount of cassiterite is also detected in the green enamel of knife handle 28710A (635–775 cm^{-1} doublet, Figure 22) near black lines. The presence of cassiterite in artefacts typically intended for the Chinese Emperor underscores its association with high-quality production [65–67].

The spectra recorded on the Orry' plate blue overglaze with a 457.5 nm are quite similar to those obtained on the large dish. Under blue laser excitation, additional features

are observed, specifically broad bands at 1270–1280 and 2900 cm^{-1}. The first band has previously been attributed to the presence of borate [34], with borax reported in the recipes [55]. Complex resonance features may also contribute to these observations.

3.7.2. Opaque White Overglaze

Lead arsenates can form different structures depending on their composition. The best characterized is apatite, with a non-stoichiometric composition ($Na_{1-x-y/2}K_xCa_yPb_4(AsO_4)_3$ [62,63]), but other structures and compositions such as feldspars are also known [62]. Apatite typically exhibits a Raman spectrum with a narrow line around ~812 cm^{-1} and a shoulder near ~775 cm^{-1}, as observed in the large dish (Figure 21), the torch 12292, the Rothschild10 ewer (Figure 21), the Orry's plate (Figure 23), and Ellias Guillot's plates SN27A and SN27B (Figure 24). In certain blue overglazes, this phase is also present, but the As-O band is significantly broadened, indicating a more disordered structure, possibly feldspar, and/or very small crystallites formed through precipitation–nucleation at lower temperatures. If the white enamel highlights were applied last (appearing in relief), their firing likely occurred at a relatively low temperature, achievable through the addition of borax and/or increased lead content. The lower intensity of the As-O stretching mode in the overglaze blues suggests that arsenic is primarily present as an element associated with cobalt in the ingredients used, such as smalt, rather than intentionally added arsenic. These blue enamels are also expected to contain borax [34,55], a flux that includes boron, and often small amounts of sodium and lithium [69], which efficiently lower the melting temperature and enhance gloss. Therefore, these overglazes can be fired last, as seen in the thick blue enamels observed on Orry's tureen (Figure 8).

The plate attributed to Samson, however, does not use lead arsenate, suggesting a 20th century production era when lead arsenate, widely used in previous centuries, was abandoned.

3.7.3. Yellow Overglaze

A very weak signature of lead–tin yellow is detected for the large dish (low peak around ~135 cm^{-1}), as seen in the spectrum of the Orry's plate (Figure 21). The intense spectra (peaks at 140, 325 and 450 cm^{-1}) were obtained for the Rothschild10 ewer (Figure 19) and the knife handles 28710A and 28710B (Figure 20). This variation suggests that the yellow enamels were fired at different temperatures [62,70,71]. It can be assumed that the second group of artefacts (those exhibiting a 'nice' spectrum) was produced after the production of lead–tin yellow pigment was mastered in China.

Based on our experience analysing Qing enamelled porcelain [40,66–68], pieces from the Kangxi reign typically exhibit less intense Raman spectra in yellows, indicating the sparing use of the colour due to limited availability and mastery of the pigment. This observation aligns with the dating attributed to the Orry plate and large dish around ca. 1720–1730, near the end of Kangxi's reign or the beginning of Yongzheng's reign. In contrast, the ewer, torch, and knife handles show more vibrant yellow spectra, suggesting a later production period around ca. 1740–1750, consistent with the final orders placed by the *Compagnie des Indes Orientales*.

3.7.4. Green Overglaze

The spectra of green overglazes exhibit certain variability. When Cu^{2+} ions are dissolved in the network, we primarily observe the signature of a lead-rich glass, characterized by a SiO_4 stretching band at a relatively low wavenumber. For the large dish (Figure 21), this band is around 970 cm^{-1}, while for the knives (Figure 22), ewer (Figure 21), and torch (Figure 21), the SiO_4 stretching modes show two components at ~982 and 1030–1035 cm^{-1}, indicating a composition less rich in lead [64,65,72], approaching that of the yellow areas. These differences suggest varying glazing conditions, providing additional evidence for different production dates or places.

In the green overglazes of the 'Samson' plate (Figure 24), a very strong fluorescence is observed. This fluorescence serves as a secondary criterion for identifying Samson copies. In Raman analyses of other objects attributed to this manufacturer, similarly strong fluorescence of the glaze under green laser excitation has consistently been noted. We can think that in the pursuit of productivity during the 20th century, traditional barrel grinding of glaze precursor mixtures with flint pebbles was replaced by using steel balls, followed by an acid treatment to remove iron contamination from ball wear. This sequence likely introduced electronic defects that contribute to the observed fluorescence.

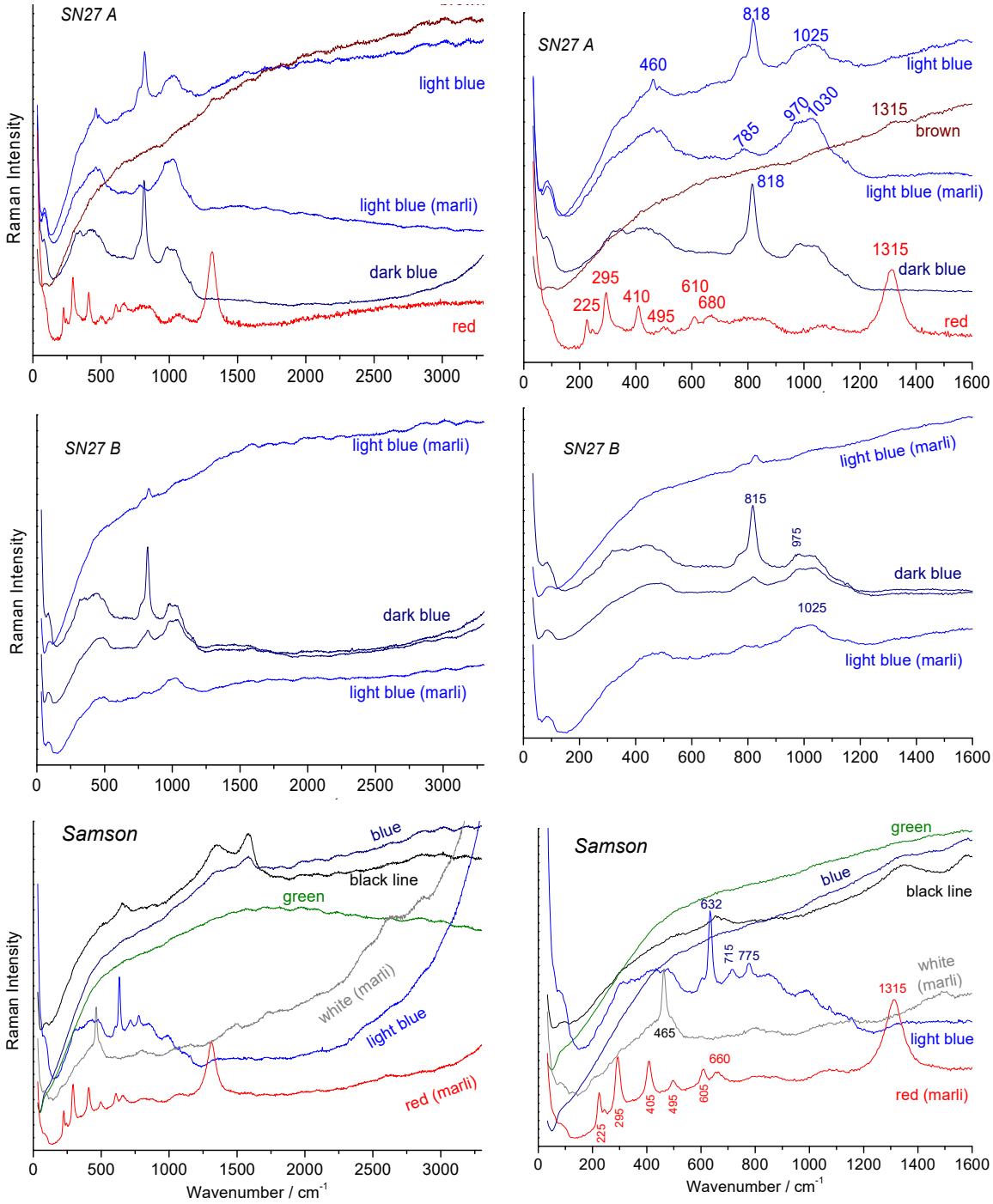

Figure 24. Representative Raman spectra recorded on various coloured areas of plates of Figure 7 with 532 nm exciting laser line (on-site analyses).

3.7.5. Red to Pink Overglaze

Two distinct types of signatures are observed: the first corresponds to the hematite phase (discussed further), while the second is characteristic of the presence of metal nanoparticles, exhibiting fluorescence with a maximum around ~550 nm (Figure 21, Rothschild10 artefact). Depending on the excitation wavelength of the laser, the spectrum of hematite varies slightly, with the resonant band (bi-magnon) around 1315 cm^{-1} showing maximum intensity under green light excitation [73,74].

Spectra of 'pure' hematite (α–Fe_2O_3, hereafter referred to as nH) displaying narrow bands around 225 and 290 cm^{-1} are recorded for the large dish, large tureen, and Orry's plate, indicating the use of pure iron oxide precursors. In contrast, broader bands (bH), accompanied by an additional small peak around 230 cm^{-1}, are observed for knives 28710A and 28710B (Figure 20) and SN27A Ellias Gillot plate. The broadening of bands suggests partial substitution of iron by another element such as titanium or aluminium [74], a phenomenon noted in various '*Chine de commande*' [34], indicating the use of two types of raw materials. Simultaneously, the signature of the opacifier lead arsenate is also observed.

The Raman spectra in Figure 25 confirm the use of different yellow pigments from the lead–tin/lead–antimony family (Naples Yellows *senso latu*). For the large dish, detecting the main peak around (or less than) 135 cm^{-1} is challenging due to several reasons: (i) a very strong Rayleigh wing, characteristic of a highly heterogeneous glaze; (ii) a low amount of pigment; and (iii) poor crystallinity. It is difficult to distinguish between these factors. These observations align with the hypothesis of a limited availability of the pigment, suggesting an early production date, as inferred from the pXRF analysis. The main components of the SiO_4 stretching mode of the glassy silicate matrix of yellow areas peak at ~990 cm^{-1} for the Orry tureen and large dish. On the contrary, an important second component is observed at ~1020 cm^{-1} for the ewer (Rotschild10), the two knife handles (MAD 28710A and 28710B), and the torch (MAD 12292), indicating a composition richer in alkali [64].

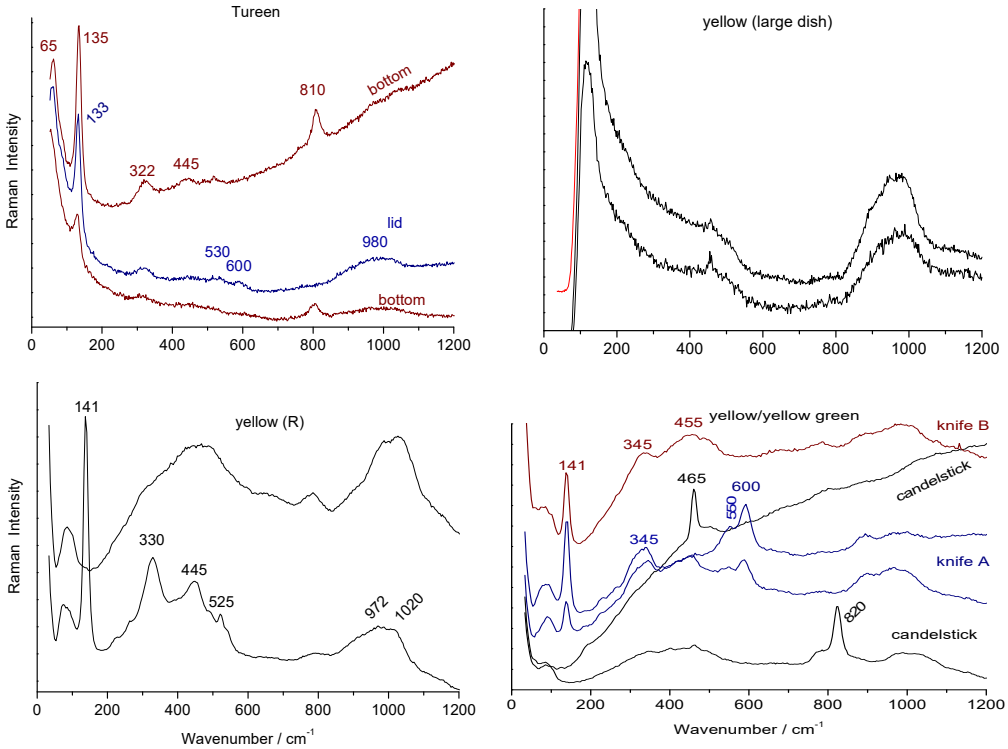

Figure 25. Representative Raman spectra recorded on various yellow areas of Orry tureen (**left**, bottom and lid), large dish (**right**), ewer (R: Rotschild10, **left**), knife handle (MAD 28710A and 28710B, **right**) and torch (MAD 12292, **right**) with 532 nm exciting laser line (on-site analyses).

The Raman signatures of other objects show a consistent strong peak at 140 cm^{-1}. Additionally, differences are noted (Figure 26) between the overglaze of the Orry's tureen body (containing lead arsenate) and its lid (arsenate-free). It is noteworthy that the spectrum from the Rotschild10 yellow area also varies, sometimes showing the pigment's signature and other times not. This variability could be attributed to the large size of the pigment grains, allowing independent recording of the pigment's contribution versus the glassy matrix (laser spot ~a few μm^2).

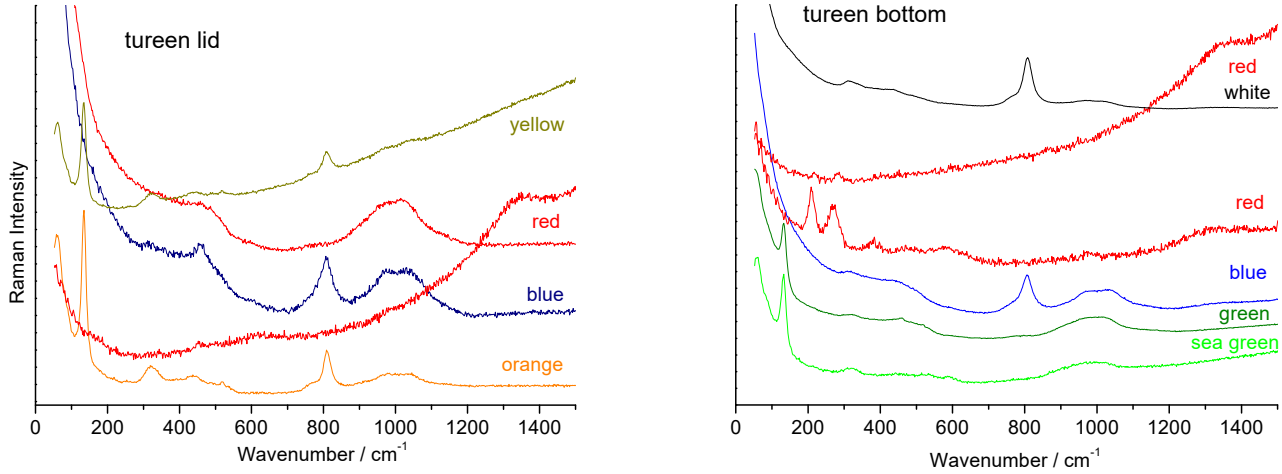

Figure 26. Representative Raman spectra of Orry tureen recorded at the laboratory with 457.5 nm exciting laser line.

4. Conclusions

The characteristics are summarized in Table 3. The inherent variability in pre-industrial ceramic production results in a dispersion of local compositions and data obtained from pXRF and Raman analyses. Good statistics should be better made with data recorded for each coloured area of objects from similar productions, which is not possible for most rare masterpieces that are exceptionally provided by their recipients/customers. Furthermore, the limited availability of analysis time for rare objects poses a significant challenge. This is why the approach focuses on identifying possible independent criteria (visual/optical properties, compositions of traces or associated elements, contamination, etc.) for the same object and comparing them. Therefore, if most of the criteria lead to an opposition, the conclusions should be reliable, whatever the limited statistics available.

A comparison of pXRF spectral signatures reveals distinct characteristics, such as Rb vs. Pb and Sr vs. Rb ratios in pastes (Figure 12), Mn vs. As (Figure 15) ratios in blue areas, and Ag vs. Au (Figure 20) in gilded areas, highlighting specific features of objects like the PP plate and the lower part of the large tureen compared to others. Notably, differences between the lid and bottom part of the large tureen are evident across multiple criteria, including paste contamination with Pb, Sr, and Rb impurity levels and Mn content in the blue overglaze.

Raman spectroscopy reveals significant differences in the signatures of yellow and greenish areas. Various types of yellow pigment are distinguished: very poorly crystallized or present in very small quantities in the large dish (main peak at 135 cm^{-1}) and the torch (125 cm^{-1}), and two well-crystallized forms, respectively, in the lower part of the Orry's tureen on the one hand (135 cm^{-1}) and the other objects on the other hand (knife handles, ewer, 140 cm^{-1}). These later yellows are richer in tin than other elements (Zn, Sb). The shift in the main peak (related to the translational vibrational mode of Pb ions) indicates different structures resulting from thermal treatment and composition. The very low intensity of this Pb mode in the yellow pigment can be considered evidence of poorly controlled pigment nucleation, suggesting an earlier production. If this criterion is accurate, it indicates that

the large dish and the torch were part of the first order made by Louis XV. The other objects would, therefore, have been made later.

The presence of cut and ground handles on the large tureen raises authenticity concerns (typically, the 18th-century tureens lack handles), suggesting that it might be a copy. This copy could have been made in China or elsewhere, considering specific paste impurities. However, more artefacts need to be studied to confirm or exclude the possibility of Chinese production iThe lid exhibits the pXRF and Raman criteria of 'good' objects like knife handles, objects less sought after and, therefore, less copied. The production to replace a non-repairable broken part copying a given decoration is, without question, part of the capabilities of the old workshops, and, therefore, a tureen body would have been made to match an older lid. We see that the visual criteria like the presence of yellow colour in certain areas of the decoration correlate with compositional variations, serving as reliable dating indicators. Unfortunately, to date, a perfectly non-invasive analysis on site does not make it possible to identify the elemental isotopic distribution, which would make it possible to better specify the uses of raw materials of the same geological origin.

The PP plate shares characteristics with the lower part of the large tureen and is considered a copy by curators; hence, it could be a production of the same origin. These objects do not present the strong fluorescence of Samson productions in Raman, so this later origin can be excluded.

Raman analysis offers fewer criteria for categorizing objects than pXRF analysis. The characteristic peaks of the crystalline phases allow for their identification. For the vitreous matrix, we provide the wavenumber of the main component of the SiO_4 stretching mode, a value that enables us to classify this matrix according to its composition (rich in lead, alkaline–lead, or alkaline) [64,65]. Only the examination of yellow areas is discriminating, as not all objects contain this colour. This is why, since no yellow overglaze spectrum was obtained from the small tureen studied in the previous work, it is not possible to link it to the groups identified in this study.

The comparative clustering of the pastes, based on the signals from Rb, Sr, and Zr impurities (Figure 27), perfectly visualizes the conclusions drawn from the XRF peak area diagrams: two types of pastes are identified, those of objects without any yellow decoration (tureen and PP plate) and others, including the tureen lid. The two-point measurement of the large dish highlights the variability in these old artisanal productions. As expected for overglaze enamels fired in an oxidizing atmosphere at Canton workshop(s), the use of imported cobalt (smalt) from Europe was required. On the other hand, underglaze blue, produced in the Jingdezhen kilns, fired in a reducing atmosphere with the porcelain body, could use traditional cobalt, rich in manganese. Lower-level classifications are meaningless, as they only differentiate each object. The clustering based on the compositions of the golden decoration (where silver is alloyed with gold and bismuth comes from the bonding flux) forms two groups, the large dish and the pot on one side and the other objects, but a measurement on another place on the large plate belongs to this second group. Is this an indication of a resumption of gilding? There are almost no pXRF studies of gilding, and, therefore, it is not possible to estimate the intrinsic variability of gilding. The construction of the clustering for the other overglazes with the impurities Rb, Sr, and Zr does not provide information, each colour forming a group due to differences in composition (arsenic for white overglaze, copper for green, iron for red). The main classification overlaps with that made using the criterion of the use of yellow overglaze.

Table 3. Main characteristics deduced from pXRF and Raman (in bracket, the crystalline phase identified and for the glassy phase the wavenumber of the main component of the stretching SiO_4 mode is given, expressed in cm^{-1}) analyses (d: disordered; v: very; w: weak; S; strong)). Expected dates in contradiction with Raman and pXRF criteria are strikethrough.

Name	View	Period	Paste (glaze)	Blue under-g	Blue over-g	White over-g	Green over-g	Yellow over-g	Red over-g	Rose over-g	Black
Large dish		ca. 1722?	F_o Fe-rich (G_o)	Mn-rich Co(U1)	Traces of Mn, Ni, Cu, As (980–1035) (d apatite) No Zn K-rich	As, Zn (apatite)	Cu Fe, Mn Sn, Zn Sb (1000)	Fe (135, vw)	Fe, Mn (hematite) nH		No peak (960)
Plate MPP		ca. 1722? Copy	F_o Rb-rich (G_o)	Mn-rich CoU1	Mn, Fe, As Cu, Zn Co-rich Ca-rich	No As No Zn		No Yellow	Fe, Au?		
Mustard pot		1725/1740?	F_o Sr-poor (G_o)	Fe-rich CoU2	Mn, Ni, As Cu, Zn High Mn K-rich	No As ? Zn	Sn, Sb Zn	Fe, Ti Sn, Sb Zn	Fe		
Philibert Orry' tureen bottom lid		ca. 1730				(apatite) (133, vS)	(135, vS) (apatite) (135, vS) (no apatite)	Pb-Sn	(hematite) nH	(apatite) (Fluo) (Nps)	(580–600)
Philibert Orry' plate		ca. 1730			(d apatite; apatite) (1270)			(133, vS)	(hematite)		
Torch 12292		ca. 1739/1740 or ca.1730?			(d apatite)	(apatite)	(apatite)	(125, vw)	(hematite)		(500–980–1035)

Table 3. *Cont.*

Name	View	Period	Paste (glaze)	Blue under-g	Blue over-g	White over-g	Green over-g	Yellow over-g	Red over-g	Rose over-g	Black
Tureen (small)		ca. 1738			(apatite) (1270)		(apatite)		(hematite)		
Tureen (large) Bottom lid		ca. 1738? Copy	$F_{1\ (body)}$ Rb-rich $F_{o\ (lid)}$ (G_K)	Fe-rich CoU2	Fe, Ni, As Mn, Cu, Zn Apatite Ca-rich	As Zn			Fe, Sn nH		580–600 (1020)
					Fe, Ni, As Mn, Cu, Zn Ca(rich)	No Zn	Sn, Sb				
Ewer Rot-child10		ca. 1725/1735			(d apatite) (980–1035)	(apatite)	(980–1035)	(140, vS) Pb-Sn		(apatite) Fluo (NPs)	No peak
Knife handle 28710A		ca. 1739/1740		rutile			(980–1040) SnO_2?	(140, vS) Pb-Sn +?Pb-Sb (+hematite)	(hematite) wH		
Knife handle 28710B		ca. 1739/1740					(980–1040)	(140, vS) Pb-Sn	(hematite) wH		
Elias Guillot' plate SN27A		ca. 1740/1743			(apatite) (980–1035)				(hematite) wH		

Table 3. *Cont.*

Name	View	Period	Paste (glaze)	Blue under-g	Blue over-g	White over-g	Green over-g	Yellow over-g	Red over-g	Rose over-g	Black
Elias Guillot' Plate SN27B		ca. 1740/1743			Apatite (980–1035)				(hematite) wH		
Plate Samson		19th c.		Fluo	SnO_2		Fluo		(hematite)		

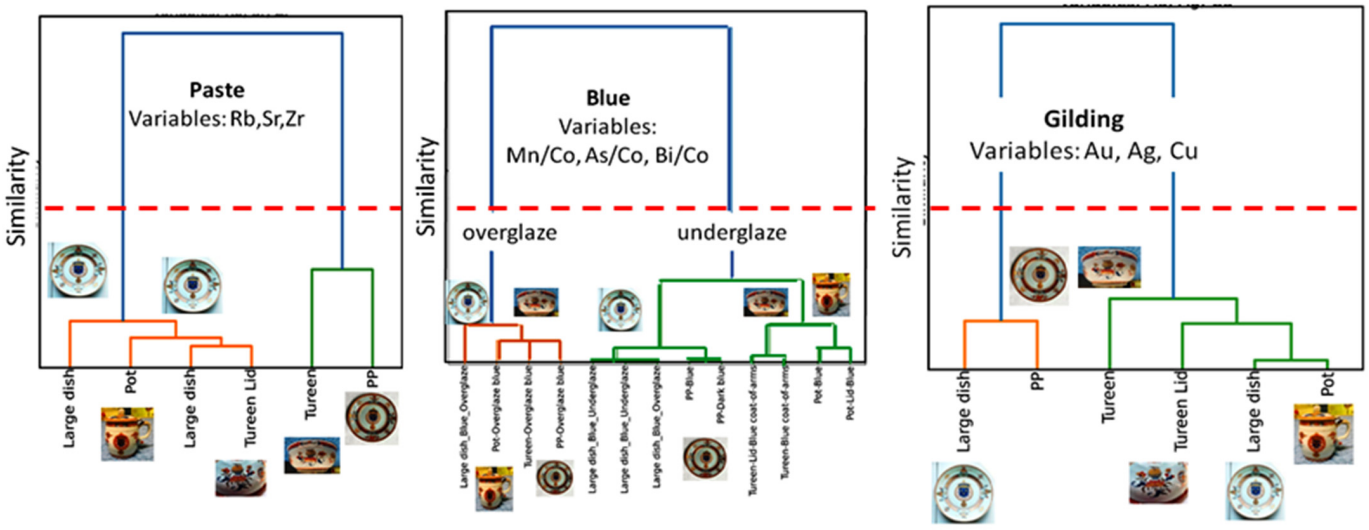

Figure 27. Hierarchical similarity diagram constructed for the comparison of pastes (variables: signals of impurities Rb, Sr and Zr), blue decorations (variables: signals of elements Mn, As and Bi normalized by that of Co) and gilding (variables: Au, Ag and Cu). The dotted line indicates the classification level considered relevant.

This work shows the full potential of on-site measurements with mobile instrumentation. It also shows its limits with the lack of statistics. However, it identifies the different parts to study, the elements to measure, and the phases whose Raman signature must be studied. The study of other objects should support the initial conclusions.

Author Contributions: Conceptualization, P.C.; methodology, P.C. and G.S.F.; investigation, P.C. and X.G.; data curation, P.C., G.S.F. and X.G.; writing—original draft preparation, P.C. and G.S.F.; writing—review and editing, P.C., G.S.F. and X.G. All authors have read and agreed to the published version of the manuscript.

Funding: This research received no external funding.

Data Availability Statement: All data are included in this paper.

Acknowledgments: The authors thank Mareike Gerken (Bruker Nano) for her help in data treatments. Béatrice Quette (Curator, Asian and Islamic Collections, Musée des arts décoratifs, Paris), Patrick Lemasson (Musée du Petit Palais—City of Paris) and the anonymous collector are thanked for the possibilities of access to the artefacts. H.G.M. Edwards is acknowledged for the editing.

Conflicts of Interest: The authors declare no conflicts of interest.

References

1. Ayers, J.; Impey, O.; Mallet, J.V.G. *Porcelain for Palaces: The Fashion for Japan in Europe 1650–1750*; Oriental Ceramic Society: London, UK, 1990.
2. Impey, O. Collecting Oriental Porcelain in Britain in the Seventeenth and Eighteenth Centuries. In *The Burghley Porcelains, an Exhibition from the Burghley House Collection and Based on the 1688 Inventory and 1690 Devonshire Schedule*; Japan Society: New York, NY, USA; Tokyo, Japan, 1990; pp. 36–43.
3. Castelluccio, S. *Le Gout pour les Porcelaines de Chine et du Japon à Paris aux XVIIe et XVIIIe Siècles*; Monelle Hayot Editions: Saint-Rémy-en-l'Eau, France, 2013.
4. van Campen, J.; Eliëns, T.M. *Chinese and Japanese Porcelain for the Dutch Golden Age*; Zwolle: Waanders Uitgevers, The Nederlands, 2014.
5. Howard, D. *Chinese Armorial Porcelain*; Faber & Faber: London, UK, 1952; Volume 1.
6. Jourdain, M.; Soame, J. *Chinese Export Art in the 18th Century*; Spring Books: Feltham, UK, 1967.
7. Le Corbeiller, C. China trade armorial porcelain in America. *Antiques* **1977**, *112*, 1124–1129.
8. Godden, G.A. *Oriental Export Market Porcelain and Its Influence on European Wares*; Grenada: London, UK; New York, NY, USA, 1979.
9. Le Corbeiller, C.; Frelinghuysen, A.C. Chinese Export Porcelain. *Metrop. Mus. Art Bull.* **2003**, *60*, 1–60. [CrossRef]

10. Howard, D.S. *Chinese Armorial Porcelain*; Heirlomm & Howard: London, UK, 2003; Volume 2, p. 155.
11. Lebel, A. *Armoiries Françaises et Suisses sur la Porcelaine de Chine au XVIIIe Siècle*; Antoine Lebel: Bruxelles, Belgium, 2009.
12. Castellucio, S. *Le Roi et la Compagnie Française des Indes Orientales, in La Chine à Versailles, Art et Diplomatie au XVIIIe Siècle*; De Rocherunne, M.L., Ed.; Somogy Editions d'Arts: Paris, France, 2014; pp. 94–119.
13. Mezin, L. *Cargaisons de Chine. Porcelaines de la Compagnie des Indes du Musée de Lorient*; Musée de la Compagnie des indes: Lorient, France, 2002.
14. Edwards, H.G.M. *Welsh Armorial Porcelain*; Springer: Cham, Switzerland, 2022.
15. Gotheborg Armorial Porcelain. Available online: https://gotheborg.com/glossary/armorial.shtml (accessed on 28 November 2021).
16. Tang, H. The finest of Earth: The English East India Company's enamelled porcelain trade at Canton during the eighteenth century. *Artefact* **2018**, *8*, 69–88. [CrossRef]
17. Castelluccio, S. Le service de porcelaine de Chine aux armes de Louis XV. *L'Objet d'Art* **2011**, *467*, 66–72.
18. Jacquemart, A. *Histoire Artistique, Industrielle et Commerciale de la Porcelaine: Sujets et Emblèmes Qui La Décorent, Marques et Inscriptions;* Qui Font Reconnaître les Fabriques d'où Elle Sort, les Variations de Prix qu'ont Obtenus les Principaux Objets Connus & les Collections où ils Sont Conservés Aujourd'hui; J. Techener: Paris, France, 1862.
19. Meyzie, P. À la table des élites bordelaises du XVIIIe siècle. *Annales du Midi* **2003**, *115*, 69–88. [CrossRef]
20. Slitine, F. C'est un vrai Samson! *Sèvres. Rev. Société Amis Musée Natl. Céramique* **1998**, *7*, 66–80. [CrossRef]
21. Albis, A.D. Saint-Cloud ou King-Te-Tchen? *Sèvres. Rev. Société Amis Musée Natl. Céramique* **2007**, *16*, 46–50. [CrossRef]
22. Available online: https://www.antikeo.com/magazine/la-manufacture-samson-une-histoire-de-famille/ (accessed on 9 July 2024).
23. Available online: https://www.rm-auctions.com/en/asian-arts-i--ii/12043-a-large-chinese-armorial-dish-from-the-service-of-king-louis-xv-of-france-yongzheng-ca-1732 (accessed on 9 July 2024).
24. Available online: https://www.christies.com/en/lot/lot-5865666 (accessed on 9 July 2024).
25. Available online: https://www.rm-auctions.com/en/asian-arts-i--ii/12212-a-pair-of-large-chinese-armorial-dishes-from-the-service-of-king-louis-xv-of-france-yongzheng-ca-1732 (accessed on 9 July 2024).
26. Available online: https://www.rm-auctions.com/en/asian-arts-i--ii/11632-three-round-chinese-armorial-tureens-and-covers-from-the-service-of-king-louis-xv-of-france-yongzheng-ca-1732 (accessed on 9 July 2024).
27. Available online: https://drouot.com/fr/l/15156403-chine-compagnie-des-indes-xvii (accessed on 9 July 2024).
28. Available online: https://www.pinterest.fr/pin/galerie-theoreme-on-instagram-porcelaines-provenant-du-service-command-pour-le-roi-louis-xv-en-chine-pour-les-petits-appartements-du-chteau--467600373820395743/ (accessed on 9 July 2024).
29. Available online: https://www.pinterest.cl/pin/367395282101798154/ (accessed on 9 July 2024).
30. Available online: http://www.cyrillefroissart.com/fr/fiche.php3?id_article=4133 (accessed on 9 July 2024).
31. Available online: https://fi.pinterest.com/pin/467600373814800871/ (accessed on 9 July 2024).
32. Available online: https://www.coronariauctions.com/en/online-only-asian-arts/4103-two-coolers-with-arms-of-king-louis-xv-of-france-in-the-chinese-export-porcelain-style-samson-paris-19th-c (accessed on 9 July 2024).
33. Available online: https://toboganantiques.com/en/objets/samson-cie-important-planter-and-its-dish/ (accessed on 9 July 2024).
34. Colomban, P.; Ngo, A.-T.; Fournery, N. Non-invasive Raman analysis of 18th Century Chinese export/armorial overglazed porcelain: Identification of the different enameling techniques. *Heritage* **2022**, *5*, 233–259. [CrossRef]
35. Available online: https://www.galerienicolasfournery.fr/collection/paire-de-petits-plats-aux-armes-de-philibert-orry-de-vignOrry-controleur-general-des-finances-en-porcelaine-de-chine-depoque-yongzheng/ (accessed on 28 August 2024).
36. Orry Christies. A Set of French Market Armorial Dishes. Available online: https://www.christies.com/en/lot/lot-6187628 (accessed on 12 November 2021).
37. Joulie, F. Philibert Orry: Directeur général des Bâtiments du roi et collectionneur. *Bull. Cent. Rech. Château Versailles* **2015**, *1*. [CrossRef]
38. Available online: https://fr.wikipedia.org/wiki/Philibert_Orry (accessed on 9 July 2024).
39. Available online: https://www.galerienicolasfournery.fr/collection/rare-assiette-aux-armes-des-guillot-pour-le-marche-hollandais-en-porcelaine-de-chine-depoque-qianlong/ (accessed on 9 July 2024).
40. Colomban, P.; Simsek Franci, G.; Gironda, M.; d'Abrigeon, P.; Schumacher, A.-C. pXRF Data Evaluation Methodology for On-Site Analysis of Precious Artifacts: Cobalt Used in the Blue Decoration of Qing Dynasty Overglazed Porcelain Enameled at Customs District (Guangzhou), Jingdezhen and Zaobanchu (Beijing) Workshops. *Heritage* **2022**, *5*, 1752–1778. [CrossRef]
41. d'Albis, A. La Marquise de Pompadour et la manufacture de Vincennes. *Sèvres. Rev. Société Amis Musée Natl. Céramique* **1992**, *1*, 52–63.
42. Available online: https://xrfcheck.bruker.com/InfoDepth (accessed on 9 July 2024).
43. Burlot, J.; Gallet, X.; Simsek Franci, G.; Bellot-Gurlet, L.; Colomban, P. Non-Invasive On-site pXRF Analysis of Coloring Agents, Marks and Glazes: Variability and Representativity of Measurements on Qing porcelain. *Colorants* **2023**, *2*, 42–57. [CrossRef]
44. Kissin, S.A. Five-element (Ni-Co-As-Ag-Bi) veins. *Geosci. Can.* **1992**, *19*, 113–124. Available online: https://journals.lib.unb.ca/index.php/gc/article/view/3768/4282 (accessed on 28 August 2024).

45. Colomban, P.; Kirmizi, B.; Simsek Franci, G. Cobalt and Associated Impurities in Blue (and Green) Glass, Glaze and Enamel: Relationships between Raw Materials, Processing, Composition, Phases and International Trade. *Minerals* **2021**, *11*, 633. [CrossRef]
46. Van Pevenage, J.; Lauwers, D.; Herremans, D.; Verhaeven, E.; Vekemans, B.; De Clercq, W.; Vincze, L.; Moens, L.; Vandenabeele, P. A combined spectroscopic study on Chinese porcelain containing Ruan-Cai colors. *Anal. Methods* **2014**, *6*, 387–394. [CrossRef]
47. Giannini, R.; Freestone, I.C.; Shortland, A.J. European cobalt sources identification in the production of Chinese Famille Rose porcelain. *J. Archaeol. Sci.* **2016**, *80*, 27–36. [CrossRef]
48. Norris, D.; Braekmans, D.; Shortland, A. Emulation and technological adaptation in late 18th-century cloisonné-style Chinese painted enamels. *Archaeometry* **2022**, *64*, 951–968. [CrossRef]
49. Wen, R.; Wang, C.S.; Mao, Z.W.; Huang, Y.Y.; Pollard, A.M. The chemical composition of blue pigment on Chinese blue-and-white porcelain of the Yuan and Ming Dynasties (AD 1271–1644). *Archaeometry* **2007**, *49*, 101–115. [CrossRef]
50. Burlot, J.; Vangu, D.; Bellot-Gurlet, L.; Colomban, P. Raman identification of pigments and opacifiers: Interest and limitation of multivariate analysis by comparison with solid state spectroscopical approach. I. Lead-tin and Naples yellow. *J. Raman Spectrosc.* **2024**, *55*, 161–183. [CrossRef]
51. Montanari, R.; Colomban, P.; Alberghina, M.F.; Schiavone, S.; Pelosi, C. European Smalt in 17th-Century Japan: Porcelain Decoration and Sacred Art. *Heritage* **2024**, *7*, 3080–3094. [CrossRef]
52. Colomban, P.; Calligaro, T.; Vibert-Guigue, C.; Nguyen, Q.L.; Edwards, H.G. Dorures des céramiques et tesselles anciennes: Technologies et accrochage. *ArcheoSci. Revue d'Archéométrie* **2005**, *29*, 7–20. [CrossRef]
53. Hunt, L.B. The true story of Purple of Cassius: The birth of gold-based glass and enamel colours. *Gold Bull.* **1976**, *9*, 134–139. [CrossRef]
54. Lichota, L.; Michalski, M.Z. Technological Aspects of Polish Colored Glass Tableware Manufacturing in the Second Half of the 18th Century. *J. Glass Stud.* **1997**, *39*, 83–91. Available online: https://www.jstor.org/stable/24190166 (accessed on 28 August 2024).
55. Maggetti, M.; d'Albis, A. Phase and compositional analysis of a Sèvres soft paste porcelain plate from 1781, with a review of early porcelain techniques. *Eur. J. Mineral.* **2017**, *29*, 347–367. [CrossRef]
56. Colomban, P.; Simsek Franci, G.; Gerken, M.; Gironda, M.; Mesqui, V. Non-Invasive On-Site XRF and Raman Classification and Dating of Ancient Ceramics: Application to 18th and 19th Century Meissen Porcelain (Saxony) and Comparison with Chinese Porcelain. *Ceramics* **2023**, *6*, 2178–2212. [CrossRef]
57. Geyssant, J. Bernard Perrot (1640–1709), maître de la verrerie d'Orléans. Ses innovations dans le contexte verrier européen du XVIIe siècle. *Sèvres. Revue Société Amis Musée Natl. Céramique* **2014**, *23*, 30–43. [CrossRef]
58. Colomban, P.; Kırmızı, B. Non-invasive on-site Raman study of polychrome and white enamelled glass artefacts in imitation of porcelain assigned to Bernard Perrot and his followers. *J. Raman Spectrosc.* **2020**, *51*, 133–146. [CrossRef]
59. Colomban, P.; Kırmızı, B.; Clais, J.B.; Gironda, M. An on-site Raman and pXRF study of Joseph Coteau and Philippe Parpette's jewelled porcelain: A summit of ceramic art. *J. Cult. Herit.* **2020**, *46*, 82–94. [CrossRef]
60. Colomban, P.; Gironda, M.; Simsek Franci, G.; d'Abrigeon, P. Distinguishing genuine imperial Qing dynasty porcelain from ancient replicas by on-site non-invasive XRF and Raman spectroscopy. *Materials* **2022**, *15*, 5747. [CrossRef] [PubMed]
61. Colomban, P.; Treppoz, F. Identification and differentiation of ancient and modern European porcelains by Raman macro-and micro-spectroscopy. *J. Raman Spectrosc.* **2001**, *32*, 93–102. [CrossRef]
62. Burlot, J.; Vangu, D.; Bellot-Gurlet, L.; Colomban, P. Raman identification of pigments and opacifiers: Interest and limitation of multivariate analysis by comparison with solid state spectroscopical approach. II. Arsenic-based opacifiers and relation with cobalt ores. *J. Raman Spectrosc.* **2024**, *55*, 184–199. [CrossRef]
63. Manoun, B.; Azdouz, M.; Azrour, M.; Essehli, R.; Benmokhtar, S.; El Ammari, L.; Ezzahi, A.; Ider, A.; Lazor, P. Synthesis, Rietveld refinements and Raman spectroscopic studies of tricationic lacunar apatites $Na_{1-x}K_xPb_4(AsO_4)_3$ ($0 < x < 1$). *J. Mol. Struct* **2011**, *986*, 1–9. [CrossRef]
64. Colomban, P.; Tournié, A.; Bellot-Gurlet, L. Raman identification of glassy silicates used in ceramic, glass and jewellery: A tentative differentiation guide. *J. Raman Spectrosc.* **2006**, *37*, 841–852. [CrossRef]
65. Colomban, P.; Simsek Franci, G. Timurid, Ottoman, Safavid and Qajar Ceramics: Raman and Composition Classification of the Different Types of Glaze and Pigments. *Minerals* **2023**, *13*, 977. [CrossRef]
66. Colomban, P.; Gironda, M.; Vangu, D.; Kırmızı, B.; Zhao, B.; Cochet, V. The Technology Transfer from Europe to China in the 17th–18th Centuries: Non-Invasive On-Site XRF and Raman Analyses of Chinese Qing Dynasty Enameled Masterpieces Made Using European Ingredients/Recipes. *Materials* **2021**, *14*, 7434. [CrossRef] [PubMed]
67. Colomban, P.; Simsek Franci, G.; Burlot, J.; Gallet, X.; Zhao, B.; Clais, J.-B. Non-Invasive On-Site pXRF Analysis of Coloring Agents, Marks and Enamels of Qing Imperial and Non-Imperial Porcelain. *Ceramics* **2023**, *6*, 447–474. [CrossRef]
68. Colomban, P. Tracer de façon non-invasive l'utilisation de recettes et/ou d'ingrédients européens dans les objets émaillés de la Dynastie Qing: Stratégie et premiers resultants. *Artefacts* **2023**, *18*, 161–193. [CrossRef]
69. Burlot, J.; Colomban, P.; Bellot-Gurlet, L.; Lemasson, Q.; Pichon, L. Non-invasive analyze of Boron and Lithium in 18th Century Chinese porcelain enamel and glaze: A PIXE/PIGE study. *J. Eur. Ceram. Soc.* **2024**, *44*, 116746. [CrossRef]
70. Sakellariou, K.; Miliani, C.; Morresi, A.; Ombelli, M. Spectroscopic investigation of yellow majolica glazes. *J. Raman Spectrosc.* **2004**, *35*, 61–67. [CrossRef]

71. Montanari, R.; Alberghina, M.F.; Casanova Municchia, A.; Massa, E.; Pelagotti, A.; Pelosi, C.; Schiavone, S.; Sodo, A. A polychrome Mukozuke (1624–1644) porcelain offers a new hypothesis on the introduction of European enameling technology in Japan. *J. Cult. Herit.* **2018**, *32*, 232–237. [CrossRef]
72. Simsek, G.; Geckinli, A.E. An assessment study of tiles from Topkapı Palace Museum with energy-dispersive X-ray and Raman spectrometers. *J. Raman Spectrosc.* **2012**, *43*, 917–927. [CrossRef]
73. Marshall, C.P.; Dufresne, W.J.; Rufledt, C.J. Polarized Raman spectra of hematite and assignment of external modes. *J. Raman Spectrosc.* **2020**, *51*, 1522–1529. [CrossRef]
74. Froment, F.; Tournié, A.; Colomban, P. Raman identification of natural red to yellow pigments: Ochre and iron-containing ores. *J. Raman Spectrosc.* **2008**, *39*, 560–568. [CrossRef]